7 Imaging Confocal Microscopy

Dr Roger Artigas

Sensofar Tech SL
Technical University of Catalonia (UPC)
Centre for Sensors, Instruments, and Systems Development (CD6)

Abstract

Imaging Confocal Microscopy is a well known technology for the three dimensional measurement of surface topography. A confocal microscope is used for the acquisition of a sequence of confocal images through the depth of focus of the objective. The highest signal within the images of the sequence for each pixel correlates with the height position of the topography. Confocal microscopy has many advantages like having the highest Numerical Aperture available on an Optical Profiler, meaning the highest lateral resolution and the highest measurable local slope. The field of applications is very broad, from semiconductor, materials, paper, energy, biomedical, optics, flat panel displays, etc.

This guide describes a good practice for the measurement and characterization of smooth and rough surface topography using Imaging Confocal Microscopy. The basic principle and available technologies are described along with a good practice of instrument use and limitations.

Table of contents

7.1 Basic Theory

7.1.1 Introduction to Imaging Confocal Microscopes

Confocal microscopy was invented by Marvin Minsky in 1957, but because a confocal image is generated electronically, it has not been a practical microscopy method until computers had enough processing power. The basic field of applications of confocal microscopes is for biological studies were the samples are marked with fluorophores and excited by the illumination light source. On thick biological specimens, out of focus fluorescence that reduces the contrast of the in-focus plane is blocked by means of a confocal arrangement. A high contrast image of the in-focus plane is recovered, unveiling details of the surfaces without the need to cut them. Additionally a three dimensional reconstruction of the specimens is done by scanning the sample on the axial direction.

A confocal microscope produces optically sectioned images of the sample under inspection. The basic principle to produce an optically sectioned image is by restricting the illuminated regions on the sample by means of a structured illumination pattern and observing the reflected or backscattered light by means of a second pattern identical to the illumination pattern, which blocks the light that comes from the regions of the surface out of the focal plane of the microscope's objective. The illumination and detection patterns can be a single pinhole placed on the optical axis or a set of pinholes, slits, parallel slits, or any other pattern that effectively reduces the size of the illuminated and detection regions. Independently of the geometry of the illumination and detection patterns, in-plane scanning of such patterns is needed in order to produce a complete optically sectioned image. The in-plane scanning can be done mechanically or optically and is adapted to the specific geometry of the pattern.

A number of different confocal arrangements are existing. There are different techniques for in-plane scanning, for illumination and detection patterns, and for detector arrangements. Each different configuration optimizes a given application such as maximization of light efficiency, optimization of S/N ratio, optimization of speed, simplification or reduction of hardware cost, adaptation to different excitation wavelengths, among many others. Despite the number of different configurations, a confocal microscope can be classified in one of the three following categories: Laser Scanning, Disc Scanning, and Programmable Array Scanning.

7.1.2 Working principle of an Imaging Confocal Microscope

The simplest configuration of confocal microscopy is a Laser Scanning Microscope (figure 7.1.1). On such a configuration, a pinhole is located on the field diaphragm position of the microscope and imaged onto the surface by means of the microscope's objective. The smallest illuminated spot is reached on the focal plane of the objective and is typically a diffraction limited spot. The light

reflected from the surface passes back through the objective and is imaged onto a second pinhole, called confocal aperture, placed on a conjugate position of the illumination pinhole. At the rear of the confocal aperture, there is a photo detector recording the intensity signal reflected from the surface.

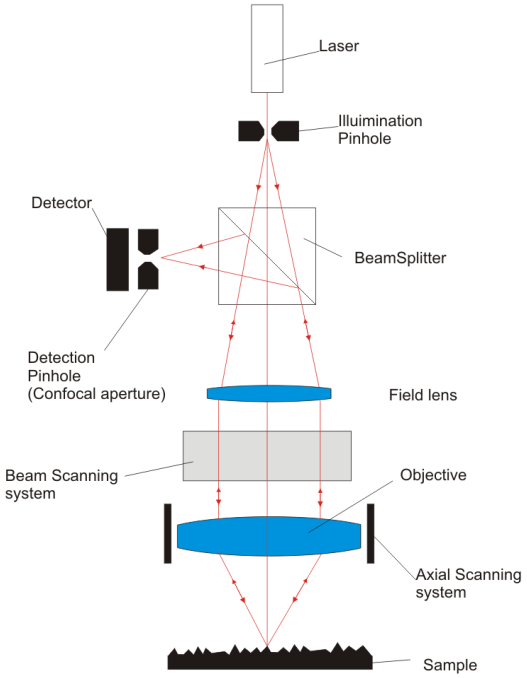

Figure 7.1.1 Basic setup of a Laser Scanning Microscope with the sample in focus position.

When the surface is placed exactly on the focal plane of the objective, the reflected light is imaged onto the confocal aperture and thus the recorded signal on the photodetector is high. On the contrary, when the surface is placed away from the focal plane of the objective (figure 7.1.2), the reflected light is imaged away from the confocal aperture. On that case, the confocal aperture filters out the light that is not coming from the focal plane of the objective and the photodetector records a lower signal.

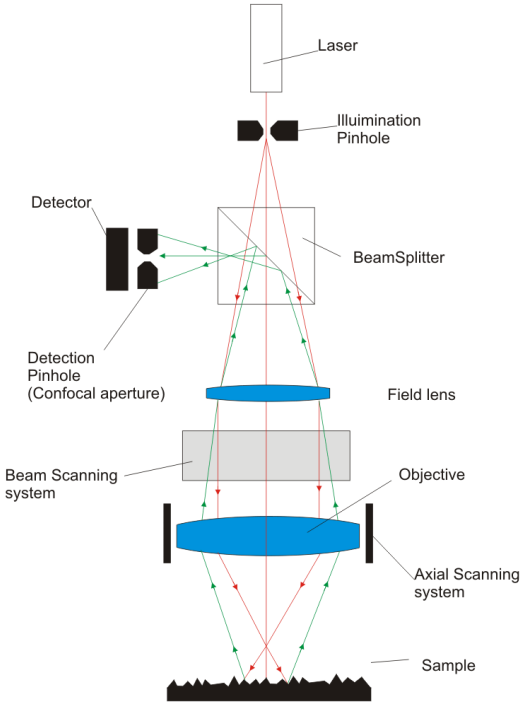

Figure 7.1.2 Basic setup of a Laser Scanning Microscope with the sample out of focus position.

A confocal image from the focal plane of the objective is recovered by scanning the beam onto the surface point by point. In a bright field image, there is signal all along the image, showing high frequency details only on that regions close to the focal plane of the objective. In contrast, in a confocal image the regions in-focus have a high signal, while the regions out of focus tend to be dark, being completely dark for those regions very far from focus. Figure 7.1.3 shows the difference between bright field and confocal images.

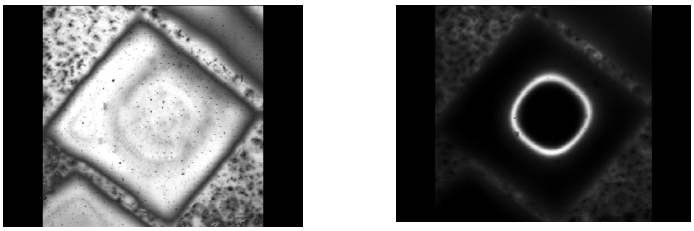

Figure 7.1.3 Bright field (left) and confocal (right) images of a laser irradiated silicon.

The basic principle of Confocal profiling relies on storing a sequence of confocal images on the memory of a computer taken from different Z planes along the depth of focus of the microscope's objective. A sequence of confocal images is shown in figure 7.1.3. An optically sectioned image shows bright grey pixel levels for those regions of the surface that lie within the depth of focus of the objective, and dark grey pixel levels for the rest of the parts of the surface that are out of focus.

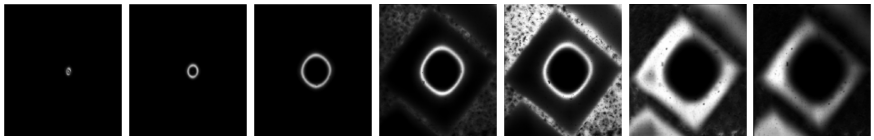

Figure 7.1.3 A series of confocal images through the depth of focus of a confocal microscope's objective.

Each pixel of the image contains a signal along the Z direction called the Axial Response similar to that shown on figure 7.1.4 (left). The maximum signal of the axial response is reached when the surface is exactly located on the focal plane of the microscope's objective. Different pixels will have the axial response maximum located on different Z positions according to the three dimensional surface shape. By locating the Z position of the maximum of the axial response for each pixel, the three dimensional surface is reconstructed. Figure 7.1.4 (right) shows the three dimensional surface calculated from the sequence of images of the figure 1.3.

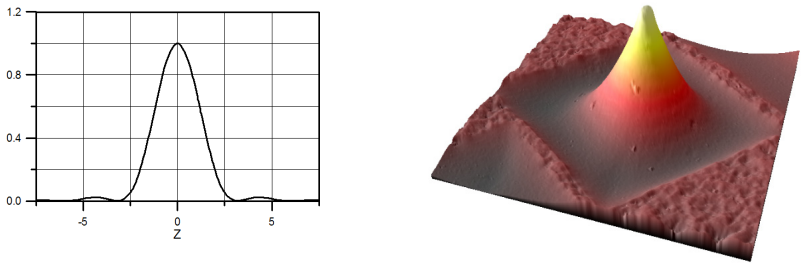

Figure 7.1.4 Left: axial response of a single pixel along the Z direction. Right: the three dimensional surface of the series of images of 1.3.

A confocal image is built up by scanning in plane (on the X or/and the Y direction) the illumination and detection patterns. Depending on the kind of confocal microscope the in-plane scanning can be very slow or very fast. A laser scanning microscope needs to scan point by point, meaning that scanning time is slow. Commercial instruments at this time reach between 1 to 5 images/second. In contrast, disc scanning and microdisplay scanning confocal microscopes are much

faster, reaching more than 10 images/second, and even more than 100 with some designs. Neither the confocal design, an in-plane scanning is needed, meaning that the sample and the focal plane of the microscope's objective should be not moving during this time. For three dimensional measurements of surfaces this means that the in-plane scanning and the axial scanning need to be synchronized in order to do not disturb each other.

Metrological algorithm

The Z location of the maximum of the axial response relates to the height location of the three dimensional surface. The fastest way to calculate the Z position is to assign it to the discrete position of the scanner. This is a low resolution method because the smallest typical step on a confocal microscope is on the order of 0.05 μm. More advanced mathematical methods are used in order to locate more precisely the metrological data. They can be classified as real time fitting algorithms and off-line fitting algorithms. A real time algorithm calculates significant mathematical data for each Z plane during the axial scan, discarding the images each time. This has the advantage of being not dependent on the computer's memory, but it has the disadvantage of not being able to deal with multiple peaks, like those appearing on thick transparent materials, among other optical artefacts. The most well known real time algorithm is the center of mass. In contrast, an off-line algorithm stores the entire series of confocal images in the computer's memory and calculates the three dimensional surface afterwards. The main advantage of an off-line algorithm is that it can deal with multiple peaks and optical artefacts, but it has the disadvantage of being limited to the computer's memory and processing time. There are several off-line algorithms. Paraboloid fitting (figure 7.1.5) uses some points around the maximum and is one the most used algorithms. It is fast, requires few data, and it can provide resolution of 1/100 the distance between Z steps. A most advanced algorithm is Gaussian fitting to the full axial response. Gaussian fitting is more precise but requires more processing time.

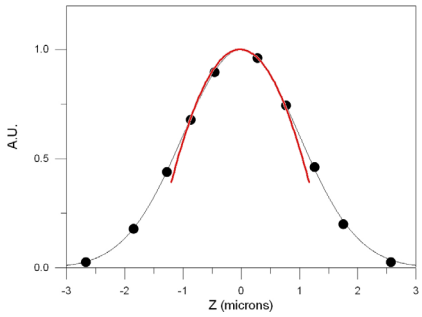

Figure 7.1.5 Paraboloid fitting to some points around the maximum of the axial response.

7.1.3 Image formation of a Confocal Microscope

7.1.3.1 General description of a scanning microscope

A scanning microscope is shown in figure 7.1.6.

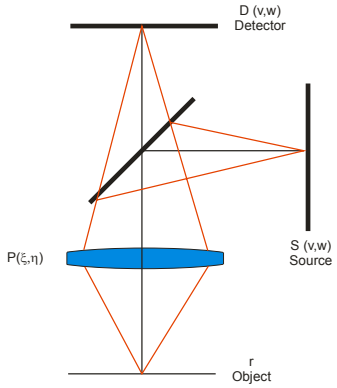

Figure 7.1.6 General layout of a scanning optical microscope

A light source pattern of distribution S(v,w) illuminates a microscope's objective with pupil function P(ξ,η). The light is focused onto the sample with reflectance distribution r and reflected back to the objective with the same pupil function and focused onto a detector with sensitivity D(v,w). The intensity on a single point of the detector with incoherent propagation is given by

$$I(u,v,w)=\int_{\infty}^{\infty}\int_{-\infty}^{\infty}D(v,w)\,t(u,v',w')\left|h(0,v-v',w-w')\right|^2 dv'\,dw' \quad (7.1.1)$$

where t(u,v',w') is the projection pattern out of focus by a quantity u, diffraction limited on the object plane, u/2 being the distance between the surface and the object plane

$$t(u,v',w')=\int_{-\infty}^{\infty}\int_{\infty}^{\infty}S(v'',w'')\left|h(u,v'-v'',w'-w'')\right|^2 dv''\,dw'' \quad (7.1.2)$$

where h(u,v,w) the fourier transform of the pupil distribution

$$h(u,v,w)=\int_{-\infty}^{\infty}P(\xi,\eta)e^{i(\xi v+\mu w)}e^{i\Delta W(u,v,w)}d\xi d\eta \quad (7.1.3)$$

and v and w the normalized optical coordinates

$$v = \frac{2\pi}{\lambda} x\, sin(\alpha)$$
$$w = \frac{2\pi}{\lambda} y\, sin(\alpha) \tag{7.1.4}$$

sin(α) is the Numerical Aperture of the objective, ξ and η the pupil coordinates normalized to the aperture radius of the pupil ξ=x/a i η=y/a, and ΔW(u,v,w) is the wavefront including focusing and aberration terms.

7.1.2 can be expressed as a convolution by

$$t(u,v,w) = S(v,w) \otimes \left|h(u,v,w)\right|^2, \tag{7.1.5}$$

resulting in a simplified expression of 7.1.1 as

$$I(u,v,w) = \left(S(v,w) \otimes \left|h(u,v,w)\right|^2\right)\left(D(v,w) \otimes \left|h(0,v,w)\right|^2\right) \tag{7.1.6}$$

On a circular pupil like those present on the microscope's objectives

$$\xi = \rho \sin(\theta) \tag{7.1.7}$$

$$\eta = \rho \sin(\theta)$$

the expression 7.1.3 simplifies to

$$h(u,v) = \int_0^1 P(\rho) J_0(v\rho) e^{i\Delta W(u,\rho)} \rho d\rho \tag{7.1.8}$$

where $J_o(x)$ is a first order Bessel function of the first type. The defocus term for the wavefront in the pupil region is expressed as

$$\Delta W(u,\rho) = -\frac{1}{2} u \rho^2 \tag{7.1.9}$$

where

$$u = \frac{8\pi}{\lambda} z\, sin^2(\alpha/2) \tag{7.1.10}$$

and 7.1.8 simplifies to

$$h(u,v) = \int_0^1 P(\rho) J_0(v\rho) e^{-i\frac{1}{2}u\rho^2} \rho d\rho \tag{7.1.11}$$

7.1.3.2 Point Spread Function (PSF) for the limiting case of an infinitesimally small pinhole

From equation 7.1.6, a single point illumination S and extended detector D will give an intensity distribution of a bright field microscope

$$I(v,w) = \left\{ \frac{2J_1\left(\sqrt{v^2+w^2}\right)}{\sqrt{v^2+w^2}} \right\}^2 \tag{7.1.12}$$

In contrast, on a confocal microscope for the limiting case of infinitesimally small pinholes, the light source distribution S and detector distribution D approximate a Dirac delta function, giving

$$I(v,w) = \left\{ \frac{2J_1\left(\sqrt{v^2+w^2}\right)}{\sqrt{v^2+w^2}} \right\}^4 \tag{7.1.13}$$

Equations 7.1.12 and 7.1.13 are shown on figure 7.1.2 where it is seen that both equations have the same zero location but on the confocal case the width is 7.1.4 times narrower than the bright field case.

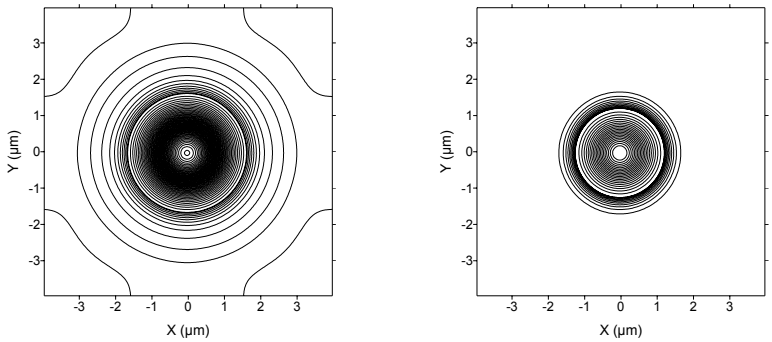

Figure 7.1.7 Intensity distribution of the PSF for a bright field microscope (left) and confocal microscope (right) for the limiting case of infinitesimally small pinholes.

Analogous, the defocus distribution of equations 7.1.12 and 7.1.13 are shown in figure 7.1.3

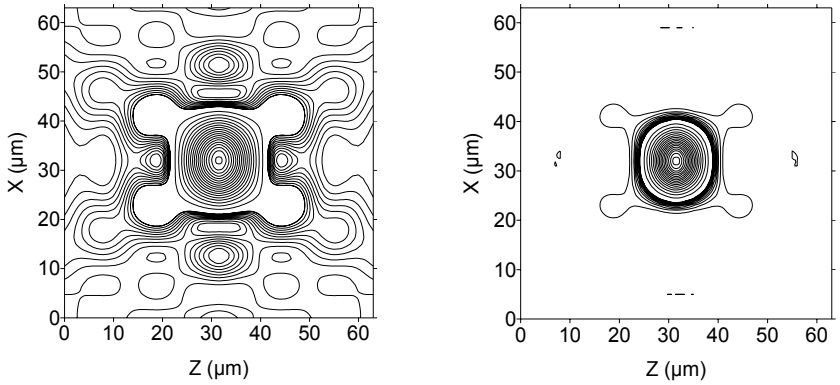

Figure 7.1.8 Intensity distribution of a bright field microscope (left) and confocal microscope (right) for the limiting case of infinitesimally small pinholes along the X-Z plane. Note the optical sectioning strength of a confocal microscope, which reduces the signal for the out of focus regions.

7.1.3.3 Pinhole size effect

7.1.3.3.1 Pinhole size effect on lateral resolution

It is intuitive to think that increasing the size of the confocal aperture will cause the signal distribution to broaden from a purely confocal microscope to a bright field microscope.

Figure 7.1.9 shows the Half Width Intensity of the PSF ($v_{1/2}$) versus the normalized radius of the detection pinhole (v_p). The pinhole diameter is normalized to a reference unit called Airy Unit (AU). The Airy Unit corresponds to the diameter of a diffraction limited spot on the objective's plane. It is well shown how the confocality is lost by increasing the size of the pinhole and the half width intensity degrades to that of a bright field microscope. The figure also shows how the half intensity is kept constant for a pinhole radius smaller than 0.5, which means that 0.5 AU is a good pinhole size to keep good confocality and maximize the detector signal.

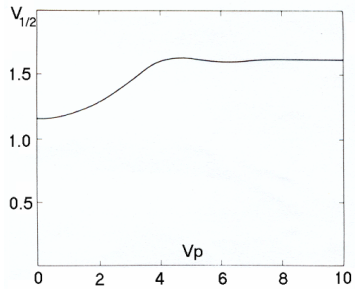

Figure 7.1.9 Half Width Intensity of the PSF versus normalized Pinhole Radius.

On confocal microscopes it is theoretically possible to close down the pinhole to very small diameters. Nevertheless, for pinhole sizes smaller than 0.25AU additional diffraction effects on the pinhole should be taken into account. This is called **wave-optical confocality**. Additionally in that case, the optical propagation of the system is coherence and the phase of the wavefront should be taken into account. For pinhole sizes larger than 0.25AU the propagation is incoherence and the diffraction can be avoided. In that case the behaviour is totally geometric and called **geometric-optical confocality**.

The lateral resolution of a confocal microscope is determined by

Geometrical-optical confocality	Wave-optical confocality	
$\frac{0.61\lambda}{NA}$	$\frac{0.37\lambda}{NA}$	(7.1.14)

7.1.3.3.2 Pinhole size effect on the axial response

The size of the detection pinhole determines the Optical Sectioning strength of a confocal microscope. The larger the pinhole size, the lower the optical sectioning. The intensity along the defocus is expressed by

$$I(u) = \left(\frac{sin(u/2)}{u/2} \right)^2 \tag{7.1.15}$$

where the normalized defocus coordinate u is related to the real defocus z by

$$u = \frac{8\pi}{\lambda} z \, sin^2(\alpha/2) \tag{7.1.16}$$

Figure 7.1.10 shows the effect of increasing the pinhole size on the axial response.

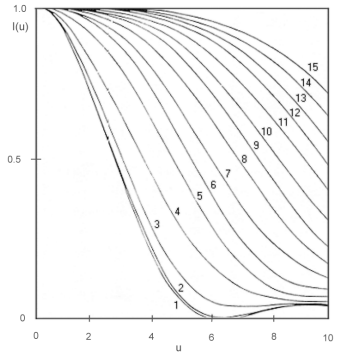

Figure 7.1.10: Axial response for different pinhole sizes. The number identifying each curve indicates the pinhole diameter expressed in Airy Units.

It is worth noting that the pinhole size (d) is described in the object plane. To obtain this value it is needed to multiply the v_p value by the magnification between the optical system and the detector. This means that in order to have pinhole sizes less than 0.5AU the following condition must be accomplished:

$$d \leq \frac{0.61\lambda}{NA} \left(\frac{M}{2} \right) \tag{7.1.17}$$

where M is the magnification of the objective and d the real diameter of the pinhole. It is also worth noting that changing the objective on the system changes the Magnification and the Numerical Aperture, and thus changes the degree of confocality.

Figure 7.1.11 shows theoretical results of the axial response for different pinhole sizes. The objective used was 50X 0.8NA.

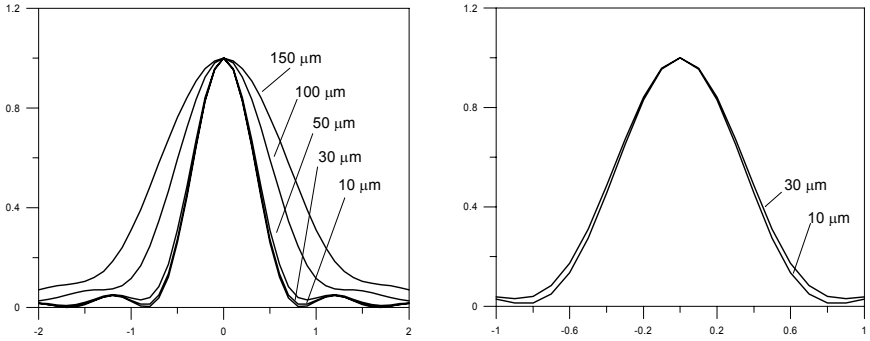

Figure 7.1.11: Axial response for different pinhole sizes. Objective 50X 0.8NA

The axial resolution of a confocal microscope is determined by

Geometrical-optical confocality	Wave-optical confocality	
$\sqrt{\left(\frac{0.88\lambda}{1-\sqrt{1-NA^2}}\right)^2+\left(\frac{\sqrt{2}\,PH}{NA}\right)^2}$	$\frac{0.64\lambda}{1-\sqrt{1-NA^2}}$	(7.1.18)

being PH the size of the detection pinhole.

7.2 Instrumentation

There are tens of different commercial confocal microscopes on the market for biological applications. Nevertheless, only few of them are purposely designed for three dimensional measurements of surfaces. Figure 7.2.1 shows some available commercial instruments based on different technologies.

Figure 7.2.1 Some commercial Confocal instruments. Clockwise: nanofocus (disc scanning), Sensofar (Microdisplay Scanning) and Olympus (Laser Scanning).

7.2.1 Types of Confocal microscopes

7.2.1.1 Laser Scanning Confocal Microscope (LSCM) configuration

Laser Scanning Confocal Microscopes are based on the basic idea of Marvin Minsky. The illumination and detection patterns are single pinholes placed on optically conjugate planes. The beam of the illumination pinhole is scanned on a raster scan onto the sample in order to build up a confocal image. Figure 7.2.2 shows the basic characteristics of a LSCM. A laser beam illuminates a pinhole placed on the field diaphragm position of the objective by means of a field lens. The image of the pinhole is formed onto the sample on the focal plane of the objective. The light reflected or backscattered from the sample passes back through the objective and is imaged onto a second pinhole called confocal *aperture* placed on a conjugate position of the illumination pinhole. A detector on the rear of the confocal aperture records the signal reflected from the surface. Light reflected from out of focus positions reaches the confocal aperture plane with out of focus image, meaning low signal at the detection plane.

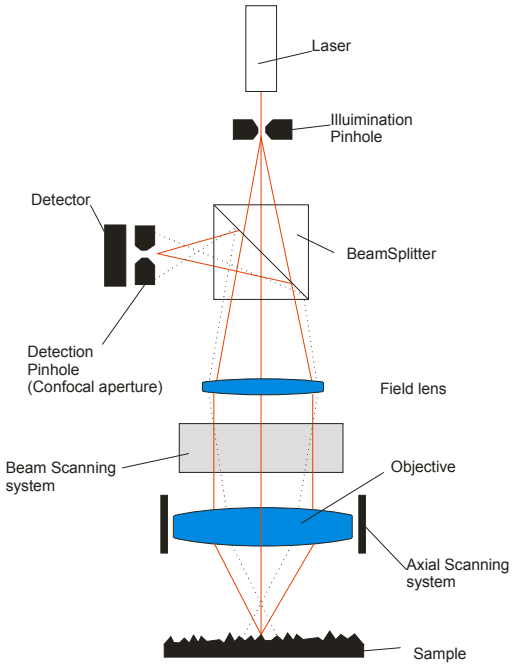

Figure 7.2.2 Typical arrangement of a Laser Scanning Confocal Microscope.

Illumination pinhole

The illumination pinhole is located on a conjugate image plane of the microscope's objective. The size of the pinhole determines the illuminated area on the surface, which is typically a diffraction limited spot and adapted to the Numerical Aperture and magnification of the objective.

Some LSCM microscopes use slit scanning instead of pinhole scanning. This has the advantage of signal and speed increase, although a loss in sectioning strength in the direction parallel to the slit is lost.

Light source

The light source on a LSCM is a Laser. For biological confocal microscopes, the wavelength of the laser is adapted to the excitation of a given fluorophore. In contrast, for three dimensional measures of technical surfaces, the wavelength is typically chosen as short as possible. Solid state diode lasers on the violet region are increasingly common.

During the beam scanning to reconstruct a confocal image, each pixel is illuminated for only a few micro-seconds. Therefore, laser light sources are needed on a LSCM.

Confocal aperture

The confocal aperture is a second pinhole placed on a conjugate position from the illumination pinhole. The size of the confocal aperture determines the Optical Sectioning strength on a confocal microscope. The smaller the diameter, the higher the optical sectioning strength and the smaller the received signal. Increasing the size of the confocal aperture allows more signal to be detected by the detector device, but at the cost of letting out-of-focus signal to reach the detector, thus reducing the optical sectioning strength.

Detector

Photomultipliers are the most commonly used detector devices in confocal microscopes. These devices have high quantum efficiency and a wide responsivity spectrum. Other detectors used on commercial instruments are photo-diodes and avalanche photo-diodes. The analog signal from the photon detector is fed onto a computer frame grabber and synchronized with the beam scanner. In order that the frame grabber records an image, the scanner generates pixel clock pulses related to its X and Y location.

Beam scanning

The beam of the illumination pinhole is scanned in on a raster scan along the X and Y directions in order to generate a confocal image. Generally, the beam is bent by two mirrors that move in perpendicular directions. The beam scanning can fall in two categories: conventional scanners and resonant scanners.

Conventional scanners are comprised of two galvanometric mirrors moving in discrete steps. The X scanner moves in quasi continuous movement and generates the lines on the confocal image, while the Y scanner steps at lower frequency line by line. Conventional scanners have high positioning repeatability meaning low pixel jitter and high confocal image quality. In contrast, the low frequency movements of the mirrors means low frame rate.

Resonant scanners generate video rate confocal images by moving one of the mirrors in a resonant way. There are resonant galvanometer scanners that achieve some tens of KHz with sinusoidal movements, and MEMs based scanners that can achieve similar frequencies with simplification of the optical setup. Resonant scanners move in a sinusoidal way, meaning that time integration for each pixel must be adjusted to the speed of the scanner. Acousto-optical devices are also used for continuous high speed beam displacement along the X direction. The Y direction scanner is typically a galvanometric mirror moving in a saw tooth pattern.

7.2.1.2 Disc Scanning Confocal Microscope configuration

Figure 7.2.3 shows the basic schematic of a Disc Scanning Confocal Microscope. A light source is collimated and directed to a disc. The disc contains an illumination pattern (and detection pattern at the same time) like those showed on figure 7.2.4. A common disc is called Nipkow on which a set of equal-sized pinholes are arranged on an Archimedean spiral. Each one of the pinholes is imaged onto the surface by means of a field lens and the microscope's objective. The light reflected or backscattered from the surfaces for each illuminated spot passes back through the objective and the field lens and is focused on the disc onto the same pinhole. Light arising from the focal plane is well focalized on the disc surface while light from out of the focus region is focused on planes before or after the disc. Each one of the pinholes acts as an illumination and detection element at the same time. Light transmitted through the pinholes is focused onto a two dimensional detector, like a CCD camera. The disc is rotated at high speed, illuminating and filtering out-of-focus light sequentially and producing an optically sectioned image.

The main advantage of Disc Scanning confocal microscopes is the fact that confocal images are taken at high frame rates. Some commercial instruments are delivering up to 1000 images/second. In contrast, light efficiency is very low in comparison to other confocal arrangements. This is due to the low pinhole fill factor on the disc (typically between 1% and 5%). Additionally, light reflected from the first surface of the disc is directed to the imaging sensor, increasing the background level and reducing the confocal contrast. To avoid this unwanted light, a polarizer is placed in front of the disc and an analyzer in front of the detector. A quarter-wave polarizer is placed on the back side of the disc in order to let the reflected light from the surface to pass through the analyzer. This combination of polarization reduces drastically the amount of signal reaching the detector.

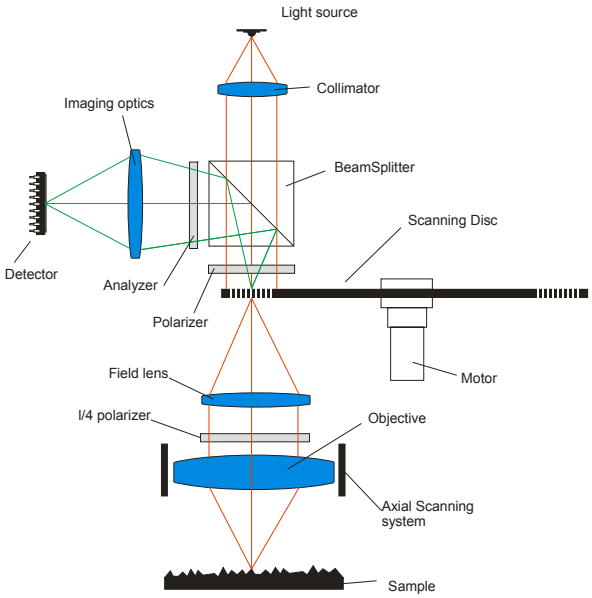

Figure 7.2.3 Typical arrangement of a Disc Scanning Confocal Microscope.

To increase the light throughput of the disc, some configurations include a disc with a microlens array placed on top of the pinhole disc. Each one of the microlenses focuses the light onto each one of the pinholes. The two discs are perfectly matched, and rotate simultaneously at high speed. This confocal arrangement can increase light efficiency up to 70%, but at the price of high manufacturing complexity. Other configurations to increase light efficiency are the use of parallel slits, like those showed on figure 7.2.4. This Slit Disc configuration has the advantage of signal increase at the price of some loss of optical sectioning strength on the direction parallel to the slits. To overcome this problem, the slits can be arranged like those on figure 7.2.4 (right image). During the rotation of the disc, each one of the pixels on the imaging detector averages all possible slit directions, averaging at the same time the loss of confocality parallel to the slit.

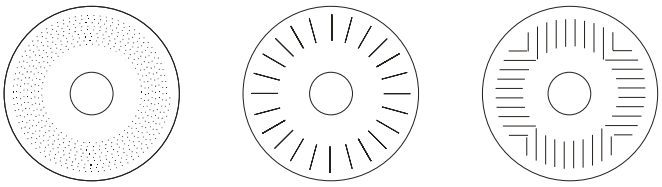

Figure 7.2.4 Three different disc pattern of a Disc Scanning Confocal Microscope. Left to right: Nipkow disc, parallel slits, point rotating slits.

Light Source

Light sources on Disc Scanning confocal microscopes can be white light sources like xenon or mercury lamps, as well as monochromatic LEDs. Laser light sources are avoided with Disc Scanning systems. The high coherence of a Laser introduces out of focus speckle that is imaged through neighbouring pinholes, increasing the noise of the confocal image.

White light sources have the benefit of producing a color confocal image in real time with color depth codification due to the chromatic aberration of the objective that focuses different wavelengths at different focal planes. This is good for surface inspection, but for three dimensional areal measurements this effect reduces the accuracy and increases the noise. The use of apochromatic objectives reduces this effect.

High power light emitting diodes (LEDs) are commonly used. A LED delivers enough power and has a nearly monochromatic spectrum. The short coherence length reduces the speckle contrast.

Scanning Disc

The most common disc is a Nipkow disc. The disc is made of glass with a layer of chrome or aluminum and a patterned pinhole arrangement. The pinholes are arranged on a spiral. The disc can have two annular regions with different pinhole sizes or different pinhole spacing. This permits the selection between optical sectioning strength vs signal. The optimum distance between pinholes to avoid crosstalk is times the pinhole diameter.

Light efficiency is increased with a microlens disc. For such arrangement a disc is made with a similar spiral pattern but with microlenses instead of pinholes. The focal plane of the microlenses is used as illumination spots and the focusing through the microlens is used back as a filter of out of focus light. The imaging detector images the pupils of the microlenses, reducing the lateral resolution.[Tiziani, Wegner, and Steudle.]

Polarization

Polarization elements are used to suppress reflected light from the upper surface of the disc and prevent it from falling onto the imaging detector.

Imaging detector

The most common imaging detector is a CCD camera, producing either an analog or a digital signal. The frame rate of the CCD camera is matched with the rotation speed of the disc in order to fulfill a confocal image. The higher the frame rate, the higher the rotation speed and the lower the overall signal. For systems to achieve

high frame rates it is typical to use cooled cameras, where noise of the camera itself is lower than the detected signal.

7.2.1.3 Programmable Array Scanning Confocal Microscope configuration (PAM)

Like Disc Scanning microscopes, Programmable Array Microscopes use parallel illumination to increase the scanning speed, the signal or both. The active element on a PAM is a microdisplay placed on the field diaphragm position of the microscope. The microdisplay is used to generate illumination and/or detection patterns.

A Programmable Array Microscope can be arranged in illumination only mode and in illumination and detection mode. In illumination only mode the pixels of the microdisplay are used to restrict the light onto the surface while the optical sectioning is achieved by the use of the pixels of a CCD camera. In contrast, in illumination and detection mode the pixels of the microdisplay are used to illuminate the surface and at the same time to filter out the light that falls out of focus.

Figure 7.2.5 shows a typical configuration of a Programmable Array Microscope on illumination only mode. The light source is collimated and directed to a microdisplay by means of a polarizing cube beamsplitter. The microdisplay is formed by a matrix of active elements that could be turned ON or OFF at high speed. The light reflected from an ON element passes trough the microscope's objective and is focused onto the sample. The light reflected or backscattered from the surface passes back through the objective and is directed to an imaging detector by means of a beamsplitter. Each element of the microdisplay correlates with one pixel of the CCD camera. To generate an optically sectioned image a set of elements of the microdisplay are turned ON, creating an illumination pattern. Each correlated pixel on the CCD records its signal. Light from out–of-focus regions fall on neighboring pixels that are not taken into account, and the signal on correlated pixels is smaller than the when the light is focused on them. A confocal image is reconstructed from a sequence of recorded images on the CCD camera correlated by shifting the ON elements on the microdisplay.

A PAM on illumination and detection mode is very similar to a disc scanning confocal microscope, where the disc is replaced by a microdisplay. Each pixel of the microdisplay acts as illumination and detection element at the same time. PAMs in illumination and detection mode are selected for high speed imaging, but suffer from low light efficiency.

The main benefit of a PAM is the fact that the illumination and detection pattern can be adapted to the surface under inspection. The illumination pattern can be a series of equally spaced elements (acting like pinholes), simulating a Nipkow disc, or a series of parallel slits, or any other pattern that effectively reduces the amount

of illuminated regions. A simple Nipkow disc can be constructed from widely spaced elements to avoid cross-talk or closely spaced elements to increase signal. A slit pattern can be adapted to surface lay structures in the perpendicular direction, increasing the detection capability for trenches.

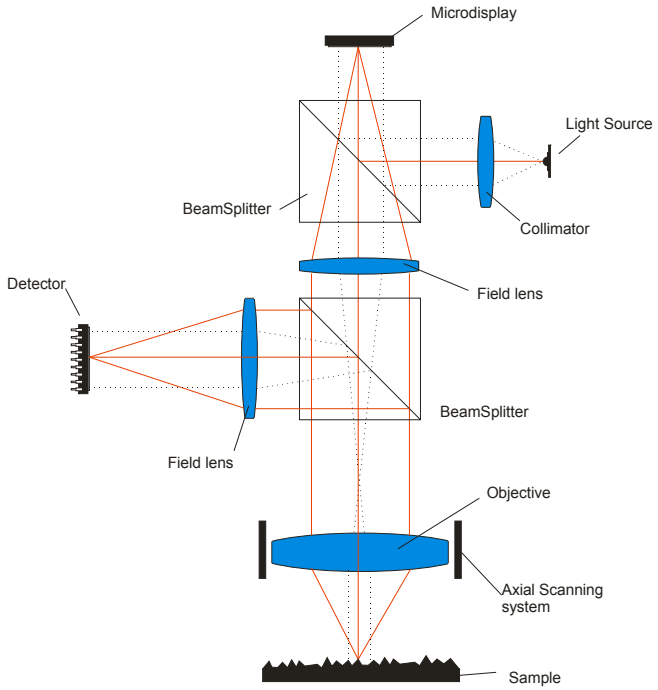

Figure 7.2.5 Typical arrangement of a Programmable Array Scanning Confocal Microscope.

Light source

The most common light sources used on PAM are monochromatic LEDs. As for on Disc Scanning systems, laser light sources introduce too much speckle due to their high degree of coherence, making them unsuitable for confocal scanning.

Microdisplay

There are many technologies for microdisplay manufacturing, although only two of them have been proven to be effective for Confocal Microscopy: Ferroelectric Liquid Crystal on Silicon (FLCoS) and Digital Micromirror Device (DMD). The reason is that image scanning has to be done at high speed, both when the microdisplay is used in an illumination and detection arrangement, or when it is only used in an illumination arrangement. Microdisplay technology can fall basically in two categories: transmission mode and reflection mode. On transmission mode, the most typical is LCD (Liquid Crystal Device). With LCD

technology each pixel can change the amount of direction of polarization according to the applied voltage. There is an entrance polarizer and output analyzer that converts the polarization state to a gray level. The biggest disadvantage of LCD technology is that it takes a few milliseconds to change from pure white to pure black, making the device rather slow for Confocal Microscopy. On reflection mode there are basically LCoS, FLCoS and DMD. LCoS microdisplays (Liquid Crystal on Silicon) are LCDs with a silicon backplane acting like a mirror. The working principle is the same as LCD but in that case the light enters and exits from the same surface. LCoS suffer from the same low speed problem of LCD making them not suitable for confocal microscopy.

FLCoS (Ferroelectric Liquid Crystal on Silicon) are the most appropriate microdisplays for Confocal Microscopy to date. The working principle is very similar to LCD, but the main difference is that the device is only stable on two polarization states. This makes the device binary by nature. The 0 polarization state is manufactured as the black point of the device, while the 90 degree polarization state is the white point. Switching time between images is a few nano-seconds, making the device very fast and able to project several thousand images per second.

DMD (Digital Micromirror Device) is a MEM based microdisplay were each pixel is a bistable mirror. They are also known as micromirrors. Each pixel has a built in mirror that can be positioned on two stable tilt positions. The optical arrangement is set up in a way that the positive stable tilt position directs light to the microscope, while the negative stable tilt position directs the light out to an absorbent material. Like FLCoS, DMD are binary by nature. The switching time is very fast, it being possible to project several thousand images per second. The optical fill factor of DMD is lower than FLCoS.

Imaging detector

The imaging detector on a PAM is a CCD camera. Like Disc Scanning systems, the camera is electronically synchronized with the microdisplay in order to fulfil a confocal image.

When the microdisplay is used in illumination and detection mode, each frame of the CCD contains a set of shifted images of the microdisplay. This means that the microdisplay is synchronized with the camera in order to show all the images within few milliseconds.

In contrast, when the microdisplay is used only for illumination, each frame of the CCD camera contains one image projected on the microdisplay. The CCD and the microdisplay are synchronized in a way that each shifted image corresponds with each recorded image, creating a sequence of images for synthetic generation of the confocal image.

7.2.2 Objectives for Confocal Microscopy

Metallographic objectives are the most used for three dimensional applications because they are designed to work on air. There are many different families intended for different applications, but the most common is to try to select the usable magnification with the highest possible Numerical Aperture. The most common objectives family used are the bright field EPI Plan APO, which has the highest aberration correction, including wavefront and colour correction. Even a confocal microscope is using a single wavelength for imaging, it is common the use of a colour camera for sample positioning and three dimensional rendering with the real texture. Plan APO objectives are available from many manufacturers from 1X to 200X magnifications with Numerical Aperture from 0.045 to 0.95. There are Extra Long (ELWD) and Super Long (SLWD) working distance objectives which are very useful for the measurement of very difficult to access surfaces. For example, a 20X magnification Super Long objective can have up to 24 mm working distance in comparison to the 4.5 mm for the Plan APO counterpart. The bad point is that the numerical aperture reduces to 0.3, which means less confocal depth discrimination and thus less signal, higher noise level and lower maximum local slope on smooth surfaces.

When measuring three dimensional surfaces with an Imaging Confocal Microscope, it is important the selection of the objective. It is recommended the use of the highest possible Numerical Aperture in order to reduce the instrument noise and keep smooth and accurate measures. In general a 50X or higher magnifications are available with 0.95 Numerical Aperture, the highest possible on a dry objective, meaning instrument noise on the order of 1 nm or less. For lower magnifications the noise is higher and the maximum local slope is lower. On such situation it is common to balance between lower magnification objective and field stitching with higher magnification. Figure 2.6 shows a Laser irradiated silicon measured with a 20X objective (0.45NA) and field stitching (625 single fields) spanning a total field of 16x16 mm^2. Such large field could not be measured with lower magnification due to the high local slopes of the bump area, which reaches more than 20 degrees local slope.

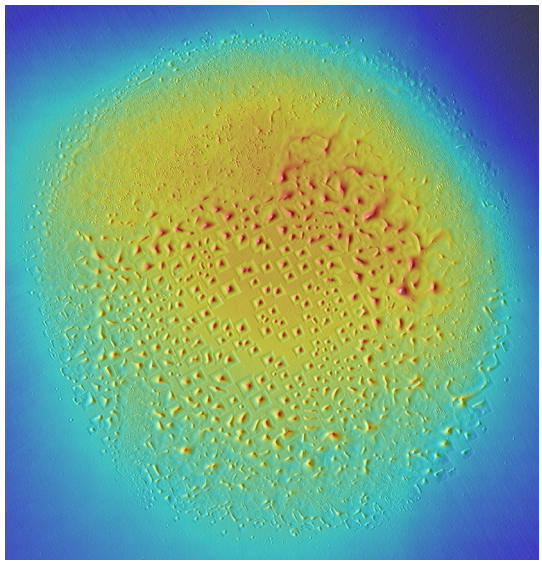

Figure 7.2.6 Laser irradiated silicon measured with a 20X objective (0.45NA) and field stitching (625 single fields) spanning a total field of 16x16 mm^2.

Figure 7.2.7 shows a part of the previous measure with a 20X magnification single field (left) and the measure on the tip with a 150X magnification (right).

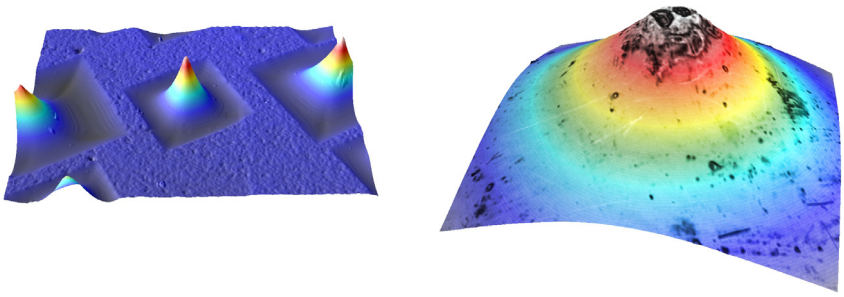

Figure 7.2.7 (Left) Single field measure with a 20X objective of a laser irradiated silicon. (Left) measure of the tip of a bump with a 150X objective.

Water immersion objectives are also available for Confocal microscopes. These objectives are constructed in a way that it is possible to dip them onto the water and image a surface that is completely immersed on it. There are many applications for the characterization of surface texture evolution under wet conditions. For example, in paper industry for paper roughness change under water, in food packaging industry for the texture evolution of film depositions of the envelopes under wet conditions or in the semiconductor industry for the surface change in wet treatments.

Collar Ring (CR) objectives are also available and very useful for some application in Imaging Confocal Microscopes. These objectives are designed to image a surface that is located on the rear of an optical window. They have a ring with marks indicating the thickness of the glass. By turning the ring to the proper number, the objective corrects the spherical aberration introduced by the optical window. A typical application of these objectives is the measure of Micro-electromechanical components (MEMs) in cryogenic conditions, where the sample is located in a freezing chamber and the device is seen through a very small window. In paper industry, it is also interesting the measure of paper roughness under pressure. On that case, the paper is pressed against a glass and the roughness is measured from the glass side.

IR and UV objectives are also used with confocal microscopes. Nevertheless, the optical design of the microscope should be adapted to the use of such wavelengths reducing the broad offer of different objectives. UV wavelength has the advantage to improve the lateral resolution close to 0.2 micron, while IR wavelength is needed for those applications imaging through silicon structures.

Despite biological objectives are also possible to be used, they are less common for three dimensional measurement of surfaces. The main benefit of them is the fact that they are oil immersion objectives. The numerical aperture is the highest possible, but at the cost of dropping oil onto the surface, loosing the “non contact” nature of confocal microscopy.

7.2.3 Vertical scanning

The vertical scanner on a confocal microscope determines the z-values of the constructed surface topography image and therefore, is the most important component for three dimensional measurements. The location in Z of the maximum of the axial response for each pixel of the image is directly related to the positioning accuracy of the Z-stage itself. Any non-linearity of the vertical scan will be embedded in the three dimensional surface measure. Typically, the vertical scanner on a confocal microscope displaces one of the three components: the sample, the objective or the full sensor. The vertical scanner can be closed-loop or open-loop.

Open-loop scanners are used for three dimensional measurements on many commercial instruments, reducing the overall cost. Although there are high quality open-loop scanners on the market, they are limited in accuracy performance.

In contrast, closed-loop scanners increase the accuracy of the measurement by incorporating a measuring device on the stage itself. On motorized stages, it is typical to incorporate an optical linear scale with a period of a few micrometers. On the other hand, piezo scanners use capacitive or piezo-resistive network sensors.

7.2.3.1 Motorized stages with Optical Linear Scales

There are many types of linear stages and actuation motors. One of the highest quality stages usable for confocal profilometry uses two parallel linear guides with recirculation balls sliders and a central ball screw. The two side sliders define the straightness and smoothness of the movement. Any deviation of straightness (pitch and yaw) will introduce relative tilt between the measurement axis and the optical axis. This tilt is called abbe error and will have a direct impact on the absolute calibration of the instrument. On the other side, the central ball screw grade will have direct relation with the accuracy of the instrument. The screw is typically actuated with a stepper motor or a servomotor with a high resolution on-axis encoder.

Optical Linear Scales are the most common devices to close loop a stage. They are are used for large travel ranges, from few millimeters up to one meter. Manufacturing tolerances of the grating and the mechanical assembly of the optical sensor on the linear scale limit the accuracy to about 1/50 of its grating period. The resolution for such measuring devices depends on the interpolation electronics and can be as high as 4000 fold less than the grating period. For a 2 micron period grating the resolution can be less than 1 nm. Despite such good resolution, a double frequency error, called quadrature error, appears within a single period of the grating, limiting the accuracy deliverable from the sensor. Figure 7.2.8 shows the accuracy error present on any Optical Scale and a table with the typical maximum error dependence on the signal period.

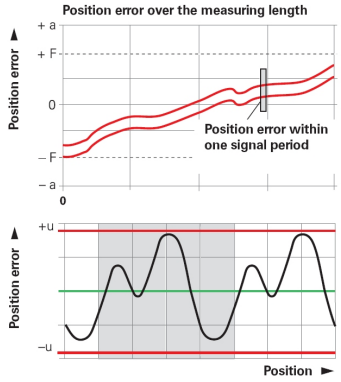

Scale signal period (μm)	Maximum error (μm)
2	± 0.02
10	± 0.1
20	± 0.2

Figure 7.2.8 Optical Linear Scale error.

The accuracy of the measure of a Step Height standard will be related to the value itself and to the starting position of the scanner relative to the linear scale. Figure 2.9 shows two cases for a 500 nm step height located at two different position of the vertical scanner: On the example the signal period is 2 microns. Each box on the figure equals to 0.5 micron height.

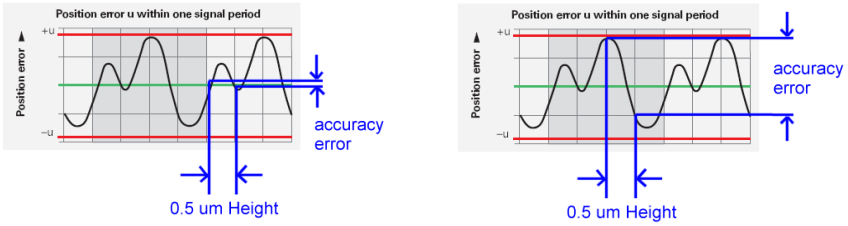

Figure 7.2.9 Accuracy error on a Step Height of 0.5 micron. Left: position of the scanner with large double frequency error of the Linear Scale. Right: position of the scanner with low double frequency error of the Linear Scale.

The left side of figure shows the step height of 0.5 micron located on a region of the linear scale were the bottom and the top parts of the step correspond to quadrature locations of the linear scale with nearly 0 difference between them. On that case, the step height value will have high accuracy. In contrast, the right side of figure 7.2.9 show the same step height located on a different position within the linear scale. On that case, the top and the bottom of the step height are located on nearly the peak to valley error of the quadrature signal error, having at the end a maximized accuracy error.

7.3.3.2 Piezo Stages

Piezo stages are non-contact stages by nature. Their construction relies on a steel or aluminum block which has been practiced a thin cut on its middle part on a spring like trajectory. That central region is the moving part and is flexure by nature. On one side of the flexure there is a piezo crystal while on the other side a position sensor. Typical travel ranges of the piezo are from few microns up to half millimeter.

Capacitive sensors and piezo-resistive sensors are able to deliver resolution below 1 nm and accuracy of less than 0.05% along its full measuring range. The noise of such sensor is even better than 0.1 nm, but it is impossible to close-loop the stage at high frequency at this resolution. Furthermore, the maximum permissible closed-loop frequency depends on the inertia mounted onto the piezo, and it should be avoided by the control electronics.

Piezo stages have the highest position accuracy and repeatability but they suffer from the maximum permissible weight. Commercial stages are able to deal with 1 Kg of maximum weight before the flexure breaks. Special designs discussed with the manufacturers of the stages are needed to hold the weight of a full sensor or a nosepiece with 6 objectives. There are also single objective piezo stages that screw directly on the position of one objective on the nosepiece. The performance of this single objectives piezo is very good, although they are not practical if the intention is to have several objectives installed on the instrument.

7.2.3.3 The Abbe error in the vertical scanning stage

The Abbe error is present on any instrument and is one of the major sources of accuracy error on a three dimensional measurement system. Figure 7.2.10 shows the typical setup of an optical profiler. The optical sensor head is mounted in a way that the sample is measured relative to the optical axis, but with height values assigned to the sensor mounted onto the stage. The stage is mounted parallel but outside of the optical axis at a distance a_z. When the stage moves it can be a relative tilt between the two axis (ϕ), introducing a measurement error Δx.

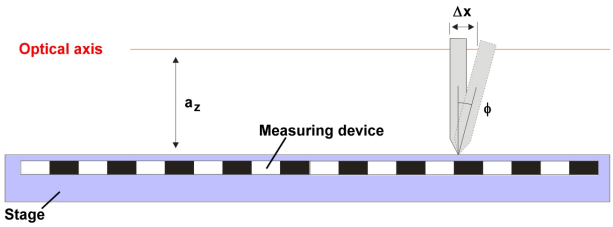

Figure 7.2.10 Typical arrangement of an optical profiler with a tilt between the scanning stage and the optical axis .

$$\Delta x = a_z \tan(\phi) \tag{2.1}$$

The accuracy error is bigger for larger distances from the vertical stage to the optical axis and for those stages with large pitch and yaw. A scanning stage with 5 μrad tilt will introduce 5 nm of accuracy error per mm separation between the scanning stage and the optical axis.

On motorized stages the tilting between the two axes follows a sinusoid trajectory with a period equal to the pitch of the ball screw. During half of the period the tilt is in one direction while on the other half is in the other direction. For those stages with high pitch and yaw the Abbe error cannot be calibrated because it depends on the portion of the ball screw where is doing the measure.

In contrast, piezo stages have a fixed tilt between the two axes and it changes only a few on a paraboloid trajectory along its full travel range. This fixed tilt can be calibrated and introduced into the software, virtually eliminating the Abbe offset error.

7.2.3.4 Comparison between motorized and piezo scanning Stages

Figure 7.2.11 shows the difference of measuring a flat mirror with a closed-loop linear stage with an Optical Linear Scale of 2 microns and a piezo scanner. The measure done with the linear stage has some non-linearities on the order of few

nm that cannot be corrected due to the inherent error of an Optical Linear Scale sensor. On the other hand, the measure done with the PZT clearly shows better results meaning better accuracy performance and higher linearity.

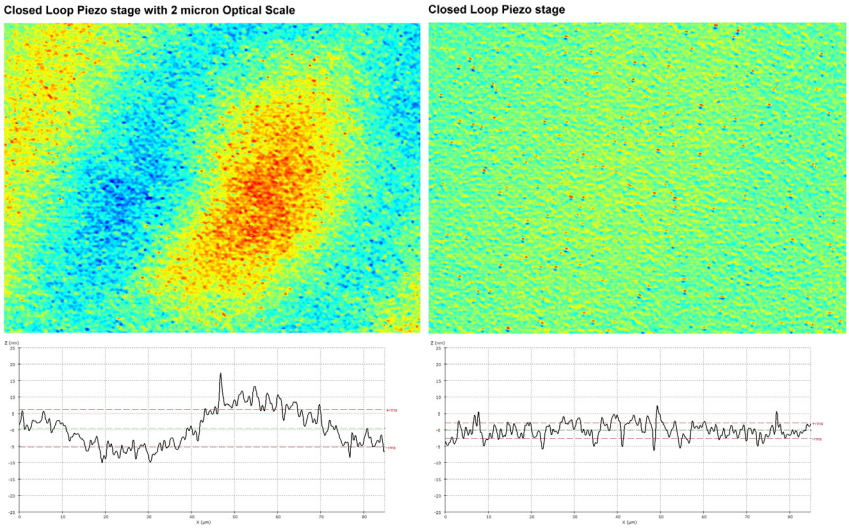

Figure 7.2.11 Measure of a high quality mirror with a closed-loop linear stage incorporating a 2 micron Optical Scale (left) and a piezo scanner with piezo-resistive network sensor (right).

7.3 Instrument use and good practice

7.3.1 Location of an Imaging Confocal Microscope

A confocal profiler is a very robust instrument with very low maintenance. Nevertheless, the environment on its location can affect seriously the performance.

The least environment requirements if for those measures that take only few seconds within a single field of view and low magnifications. For large stitching measures and the use of high magnification the external vibrations should be avoided with the use of vibration isolation tables. For measures of very smooth and flat surfaces the stability of the instrument is also very important. On that case, it is recommended that the instrument is installed on the highest possible stable conditions such as on top of a vibration isolation table isolated into a cabinet and most preferably on the ground floor of the building; avoid installing instruments on higher levels where the floor itself is acting like a membrane, introducing low frequency movements.

Cabling is also one of the main sources of instabilities on optical profilers. The cables should be exiting the instrument without introducing into it any stress. Too tightened cables or too hard cables tend to introduce external vibrations though themselves.

7.3.2 Vibration

Vibration is one of the main sources of external noise that enters onto the instrument creating non repetitive results and loss of accuracy. The vibrations are especially important for high magnifications and for long time measures such as large area stitching. The vibrations can be in somehow avoided using a vibration isolation table. There are several technologies available on the market.

- Vibration pads. These are very simple rubber pads with an internal spring that hold the full instrument. They work relatively well if the external vibration is not important at all and for the use of low magnification objectives.

- Active vibration isolation. These tables are composed by three active pads with vibration sensors and actuators that actively compensate the external vibration by pushing a plate mounted on top of them. There are many companies manufacturing active vibration, and they tend to work very well for a confocal instrument, reducing the vibration amplitude for frequencies higher than 3Hz. Nevertheless, most of the manufacturers of these tables are mounting a top aluminium plate between 10 and 20 mm thickness. During long periods of time, the top plate bends introducing very low frequency movements onto the instrument that affect the

stability of the calibration. When purchasing one of such tables it should be taken into account if the thickness of the plate will be a problem or not for the intention of use of the instrument. Thicker plates or stainless steel plates can also be mounted under request.

- Passive vibration isolation. They are composed by a top breadboard made of a sandwich of two or three stainless steel plates with thicknesses from 50 to 200 mm. Under the breadboard there are four active air legs that modify its internal pressure accordingly to the weight on top. These are the most stable tables for optical instruments. The main problem is the space needed for its installation and the necessity to have air pressure available.

7.3.3 Setting up the sample

Placement of the sample is as easy as assuring that it fits under the microscope and focusing onto its surface. Most of the commercial instruments have the possibility to show a bright field image. For rough surfaces the focusing is done very quickly and easily. In contrast, for smooth surfaces focusing is more difficult. A good help is starting with low magnification and focusing onto a dust particle, if it is available. Then change to higher magnification and change to confocal imaging. Fine focusing is now much easier and precise.

For rough surfaces or surfaces with texture, it is not very important if there is a tilt between the sample and the optical axis. For smooth surfaces it is recommended the use of a tilting stage to place the sample as perpendicular to the optical axis as possible. This assures a good matching between the measure and the calibration of the instrument and thus an accurate result.

7.3.4 Setting the right scanning parameters

Before starting to take measures it is needed to set the right scanning parameters. Some commercial instruments have automatic features that search for the optimum parameters such as scanning range, focusing and light level. For instruments in control of production this is necessary, but for instrument in research institutions it is much better to train an expert user.

Light and gain adjustment

Light level should be adjusted avoiding saturation on smooth surfaces. On rough surfaces, it is allowed to have a small percentage of saturated pixels avoiding always having big saturated regions. On some surfaces, a single light level is not enough to deal with high reflectivity and low reflectivity regions at the same time. Some commercial instruments have the option to illuminate at the same focal region with different light levels. A series of several light level sequences of

confocal images are stored and the sequence with the highest signal with no saturation is used for the topographical calculation.

The sensor gain can also be adjusted in order to highlight dark regions of the surface. Increasing the gain of the sensor also increases the noise and most of the time regions with no surface, like holes, have the signal above the threshold resulting in non trustable results like spikes or discontinuities.

Choose measurement

A confocal profiler can deal in general with single profiles, stitched profiles, single topographies and stitched topographies. Some instruments have also the option for tick film measurements of two surfaces. When selecting one of the previous options the software automatically sets for the necessary scanning parameters.

Objective

On automatic nosepieces the software recognizes the objective in use. This automatically adjusts for the optimum step size between planes and the number of planes necessary to cover the desired range. With manual nosepieces the user needs to tell the software the objective under use. When the objective used for the measurement does not match with the software, many errors appear, being the most important the mismatch of flatness error calibration (see section 4.3.1).

Area

With single field measures it is normal to choose the largest area available. On the contrary, for stitching topographies the desired area will determine how many single fields are needed. On that case, it is typical to reduce the resolution for each single field in order to keep a reasonable amount of measured pixels. For example: suppose a confocal microscope delivering single field measures with 1 Million pixels. If the desired area needs 10x10 fields this will mean 100 Million pixels measurement. For an instrument with a confocal stack image and colour image, it is needed 32 bits for the topography, 8 bits for the stack and 24 bit for colour. This means 64 bits per pixel, or 8 byte per pixel, or 800 Mb data for the full area. Imagine doing a FFT (Fast Fourier Transform) calculation on such a big file. A FFT needs auxiliary memory in a factor of 4, meaning 3.2Gb of memory. By reducing the resolution in a factor of 2 in each direction this will mean 200 Mb, much easier to handle by the software.

During field stitching some errors can occur. Alignment of the X and Y stage with the pixels of the image should be done as careful as possible. Some overlapping is used between measures and the measured data is correlated to correct for misalignments. Typical overlapping values are between 10% and 25% of the field. For highly textured surfaces a small amount of overlapping is enough. On the

contrary, for smooth surfaces with nearly no surface features it is recommended to increase the overlapping to the maximum.

Threshold

Threshold is a value that is used to assign non trustable data to missing data. The most common use of a threshold is to avoid the noise present on dark regions that will lead to spike-like data. The threshold value varies from one manufacturer to another. Some instruments are referring the threshold to a grey level, while some other use a relative number in a percentage of a fixed number.

Data interpolation

Data interpolation is used to replace non measured points for measured data with the use of interpolation algorithms. The smoothness and the final approach to the real surface profile depend on the skills of the manufacturer of the instrument to write good interpolation algorithms.

Some analysis software are able to show the profile data on red for those pixels that has been interpolated. Figure 7.3.1 shows a measure of a steel roll surface measured with low magnification. The crater region has a local slope that cannot be measured with the Numerical Aperture of the used objective, having as result non-measured regions, shown in black. The image in the right shows the restored topography.

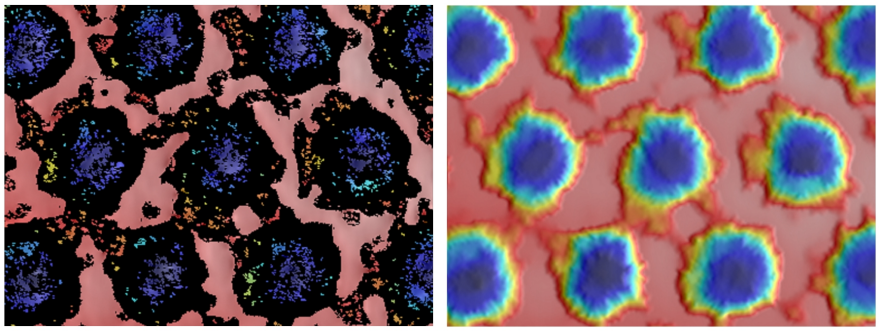

Figure 7.3.1 Measure of a steel roll with non-measured points (left) and interpolated points (right).

7.3.5 Simultaneous detection of confocal and bright field

During the axial scanning, the sequence of confocal images is stored on the computer's memory for further processing of the topography. Additionally to the three dimensional information, the confocal stack is also computed by assigning to each pixel a grey level corresponding to the highest signal within the sequence. This image is also known as the Infinite Focus image, which has all the areas in

perfect focus removing the blur images familiar with a bright field microscope. In order to get a good stack image it is very important to be sure that the image is not saturated in any point all along the axial scan. Figure 7.3.2 shows a single confocal image (left) taken with a 50X objective on an aluminium plate and the stack image (right) after processing the confocal sequence.

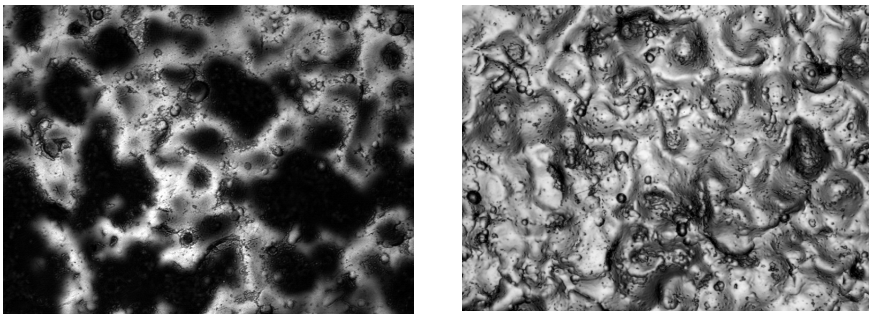

Figure 7.3.2 Confocal image (left) and confocal stack (right) of an aluminium plate.

Some confocal microscopes incorporate a colour camera additional to the confocal imaging path. The colour camera is used for sample positioning and inspection as well as for real colour texturing of the three dimensional images. During the axial scanning, a sequence of colour images is stored in parallel with the sequence of confocal images. The colour assigned for each pixel corresponds to the colour image of the Z plane where the maximum signal of the axial response is found.

On Laser Scanning instruments, a white light and a colour camera are introduced into the optical path by means of beamsplitters. On instruments using violet lasers, the white path and the violet paths are completely decoupled. In contrast, instruments using visible lasers stop the laser scanning during the acquisition of the colour image in order to do not saturate the bright field image. On Disc Scanning and Programmable array microscopes the sensor itself is a camera. Some of them use a colour camera for both, metrology and imaging, and other instruments use two cameras each one for its purpose. It is recommended the use of a monochromatic camera for metrology. A B&W camera has a better S/N signal and higher lateral resolution than a colour camera with a Bayer pattern for colour imaging which has less lateral resolution per each colour and worse pixel to pixel uniformity. A white light LED and a colour camera are introduced onto the optical path of the microscope. During the axial scanning, the confocal light source and the white light source are decoupled in order to do not over-cross them.

Acquiring simultaneously confocal and colour information makes the acquisition slower and the final measurement file larger, a serious problem for large stitching areas. Most of the times the colour information is not needed for metrological purposes, but users are not aware that the software has the colour option activated. It is highly recommended to disable the colour information except to those measures where it is really needed. Figure 7.3.3 shows a three dimensional

measure of a CCD sensor microlens array with colour height codification (left) and real colour texture (right). Note the Red, Green, and Blue filters on the microlens.

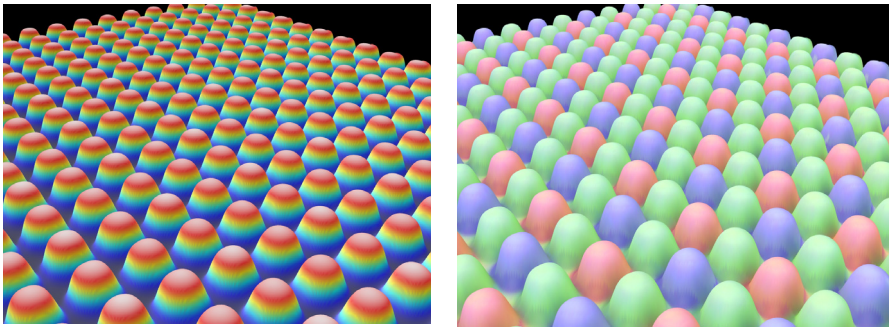

Figure 7.3.3 Topography image of a CCD sensor microlens array with colour height codification (left) and real texture colour (right).

7.3.6 Sampling

The sampling is the size of a single pixel projected onto the surface. On a Confocal Microscope, the optical design compromises between the lateral resolution of the instrument and the sampling. For medium magnification objectives (around 50X) the lateral resolution and the pixel size are more or less coincident. Lower magnifications have smaller pixel size than resolution and higher magnifications are, on the contrary, having more sampling. Typical pixel size for a 150X magnification is 0.1 micron, while the optical resolution for such an objective with a mean wavelength of 0.46 micron is 0.3 micron. This is sampling three pixels per each resolving area. Nevertheless, for Critical Dimension measurements on the lateral resolution limit it is desirable to even increase the sampling.

Some commercial instruments have the option to zoom on the confocal image. This has several utilities, although the most important is to correctly sample on the resolution limit. On Laser Scanning instruments, it is very common to have an optical zoom. The laser is scanned on a shorter area by means of the amplitude of the galvanometric mirrors or by means of a bending lens on the scanning path. This has the advantage of keeping the final number of pixels and scanning speed. With low magnification objectives the pixel size can be increased by a factor between 2X and 3X still being below the resolution limit. A 10X objective can be zoomed to emulate the magnification of a 20X or 30X while still having a sharp image, although the Numerical Aperture is kept. On the contrary, applying zoom to a high magnification objective, which already is sampled beyond the resolution limit, will make the image bigger but at the same time fuzzy. This is useful for the correct sampling beyond the resolution limit. Disc Scanning and Programmable

Array microscopes cannot use an optical zoom. Instead, they use a digital zoom on the confocal image. A digital zoom has less quality than an optical zoom, especially for low magnifications. On high magnifications a digital zoom, already zooming on an over-sampled image, has nearly the same quality of an optical zoom.

Figure 7.3.4 shows the topographical image of an AFM calibration standard with 0.66 micron period. The image on the left is under sampled with 0.1 micron per pixel, while the image on the right has a digital zoom of 6X and 0.015 micron per pixel.

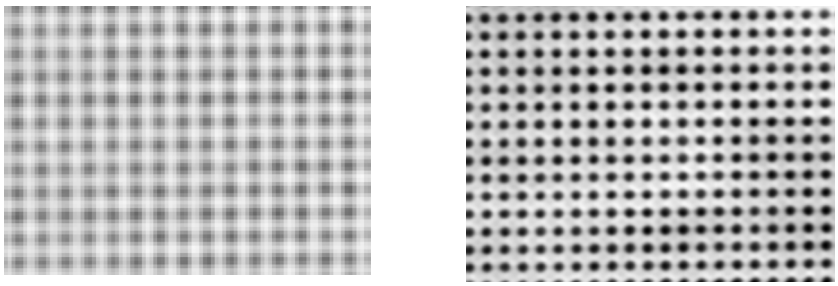

Figure 7.3.4 Under sampled (left) and correctly sampled (right) measure of an AFM calibration standard (0.66 micron pitch) with 150X magnification. The image on the right has a 6X digital zoom factor applied to the confocal images during the scan.

7.3.7 Low magnification vs. stitching

Sometimes it is important to balance between using low magnification objectives and field stitching. The use of low magnification gives large measurement area, but it inherently comes with low Numerical Aperture and thus high noise in confocal instruments. Additionally, low NA is also limiting the maximum local slope measurable on smooth surfaces, as well as on moderately rough surfaces with high wall angles. Most of the commercial instruments are equipped with XY stages for sample positioning, multiple repetitive measurements and topography stitching. In general the use of topography stitching with higher magnifications improves the result, especially when using magnifications higher than 20X. The weak point is that measurement time takes much longer and the instrument should be in better stability conditions.

Figure 7.3.5 shows the profile of a stainless steel structure with 60 degree wall slope. The black line is a single field measure with a 20X 0.45NA magnification with “spike” pixels on the slope due to low Numerical Aperture. The threshold has been lowered to 0 in order to use any signal for the calculation even on the wall region. If the threshold is set to higher levels it is possible to clean out all the spikes at the cost of having non-measured points on that region. Data interpolation

is sometimes useful for geometrical reconstruction, but the restored points cannot be used for further data analysis like profile roughness. The red line on the figure shows the measure of the same sample with a 50X 0.95NA objective, which can deal up to 72 degrees local slopes on smooth surfaces. In order to cover the full sample profile it is needed to measure three fields and stitch the result.

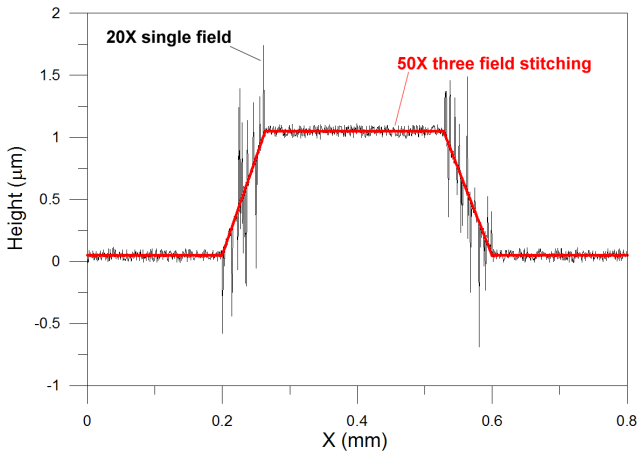

Figure 7.3.5 Profile of a stainless steel structure with 60 degree wall slope. The black line is a single field measure with a 20X magnification with "spike" pixels on the slope due to low Numerical Aperture. The red line is a three field stitching with a 50X 0.95NA objective.

7.4 Limitations of the technique

7.4.1 Maximum slope on smooth surfaces

The Numerical Aperture of the objective largely determines the maximum local slope measurable on a non-scattering surface. Figure 7.4.1 shows two typical cases where light illuminates the surface, reflects and goes back to the objective (green rays), and light that does not reach the objective (red rays). In figure 7.4.1 right is shown the limiting case where the surface tilt equals the Numerical Aperture of the objective and only the marginal ray of the objective illuminates the surface and goes back to itself. Surfaces with higher tilt do not provide any signal back.

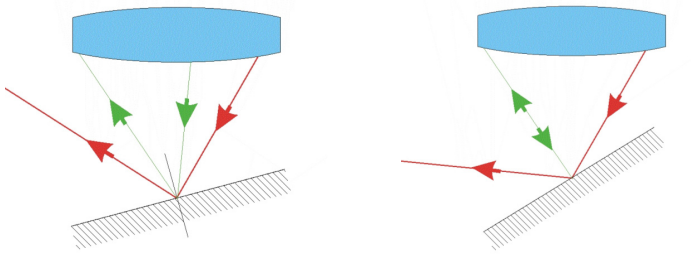

Figure 7.4.1 Surface providing signal (left) and surface with tilt equal to the numerical aperture (right) .

One of the biggest advantages of a confocal microscope is the use of high NA objectives. It is possible to use dry objectives up to 0.95NA providing a maximum measurable local surface slope up to 72 degrees. Larger slopes can be measured with higher NA objectives such as water immersion or oil immersion, although they are not practical for three dimensional measures of technical surfaces. Figure 7.4.2 shows the dependence of maximum local slope versus NA, assuming that the roughness of the surface and its propensity for scattering light in different directions is not significant.

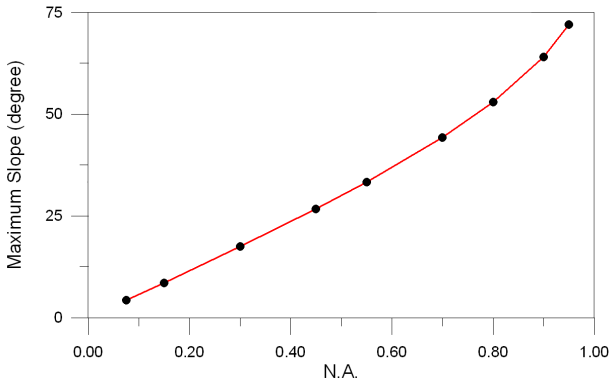

Figure 7.4.2 Maximum local slope versus objective's numerical aperture.

The mentioned limit is only applicable to optically smooth surfaces or for those surfaces with very low light scatter. For optically rough surfaces the maximum local slope could be much higher, even reaching close to a vertical step of 90 degrees.

For micro optical components with repetitive structures, such as micro prisms, there is an inherent limit called optical shadowing. Figure 7.4.3 shows a prism array with 45 degree structures. Point A and B are points on the surface where the reflected light can output the surface structure by crossing the highest point of the most neighbouring prism. Point B has a decreased effective Numerical Aperture because it is located closer to the bottom structure of the prisms. Point C is the limit point where only one ray can enter the structure, reflect perpendicularly to it and go out through itself.

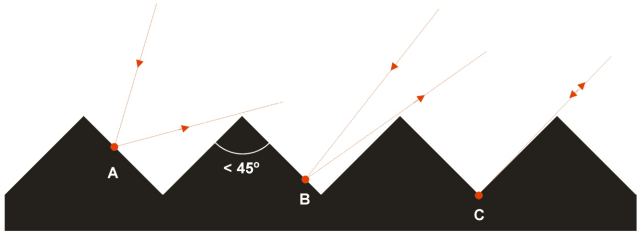

Figure 7.4.3 Prism structure with prism angle of 45 degree.

For prism structures with prism angle smaller than 45 degrees, the optical shadowing is not a problem at all, and it is possible to measure all the structure down to the bottom. In contrast, for prism structures with prism angle larger than 45 degrees, the optical shadowing appears. Figure 4.4 shows a prism array structure with 60 degree prism angle. Point A is similar to point A or B in figure 7.4.3. In contrast, Point B is the limit point where the light can enter the surface and reflect perpendicularly to itself. Any point located below point B has a shadowing effect where the light experiments several internal reflections and virtual focusing points, making any surface point below non trustable.

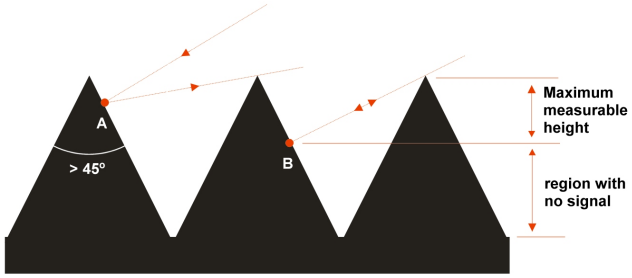

Figure 7.4.4 Prism structure with prism angle of 60 degree.

Figures 7.4.5 and 7.4.6 show the result of the measure of a 2D and 3D prism respectively with 45º and 55º prism angle. The 2D prism was measured down to the lowest point, while the 3D prism has optical shadowing.

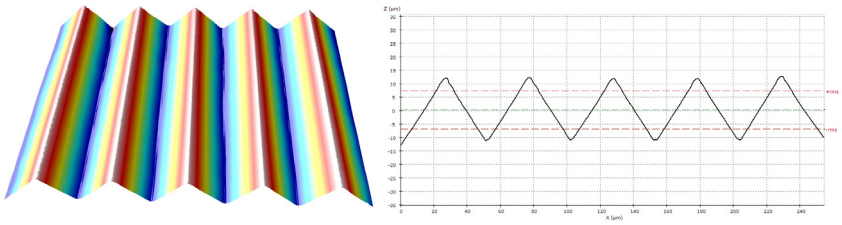

Figure 7.4.5 Measure of a 2D prism.

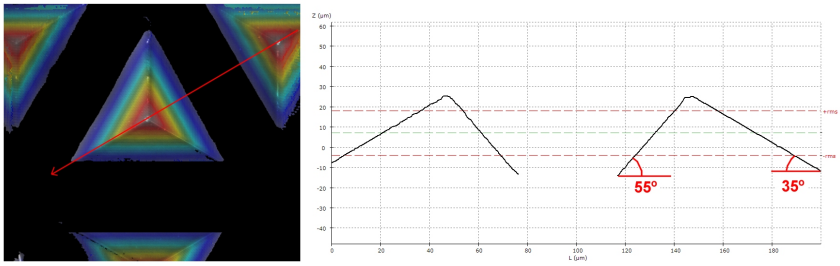

Figure 7.4.6: Measure of a 3D prism with Optical Shadowing effect.

7.4.2 Noise and resolution in Imaging Confocal Microscopes

Although the metrological algorithm increases the resolution of the Z discrete steps during the axial scan, the resolution is limited by the Numerical Aperture of the objective. The lower the Numerical Aperture, the wider the axial response. The optical slice thickness (FWHM) of a confocal microscope is approximately given by

$$FWHM = \left(\frac{0.88\lambda}{1-\sqrt{1-NA^2}} \right) \tag{7.4.1}$$

where λ is the wavelength and NA the Numerical Aperture of the objective. Figure 7.4.7 shows different axial responses for different numerical apertures with a mean wavelength of 0.55 micron.

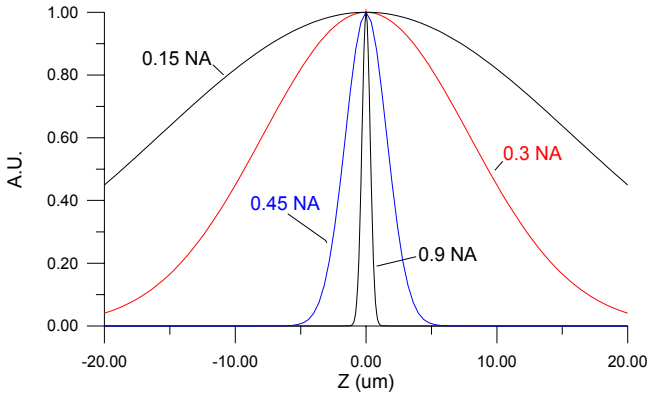

Figure 7.4.7 Axial response for different numerical apertures.

For those objectives with low Numerical Aperture, the maximum position is more difficult to locate because the signal decreases slowly. Objectives with high NA have sharper peaks and a much more precisely located maximum. The Z step between planes may be matched to the resolution of the objective. Table 7.4.1 shows some typical values.

Table 7.4.1 Optimal and conventional ranges of z-steps between confocal images during an axial scan for some numerical apertures.

Numerical Aperture	Noise limited resolution optimal step (μm)	Conventional optimal step (μm)
0.3	2.0 - 8.0	8.0 – 16.0
0.45	0.5 - 1.0	1.0 – 4.0
0.8	0.1 - 0.4	0.4 – 1.6
0.9	0.05 - 0.2	0.2 – 0.8

Making the optimal step smaller than the optimum range does not improve the noise of confocal microscopes. Figure 7.4.8 shows the dependence of the resolution of a confocal microscope on the Numerical Aperture of the objective. Low magnification objectives have typically low NA, meaning that the noise of a confocal microscope is high. For such objectives reaching 0.75 NA or larger, the noise approaches 1 nm.

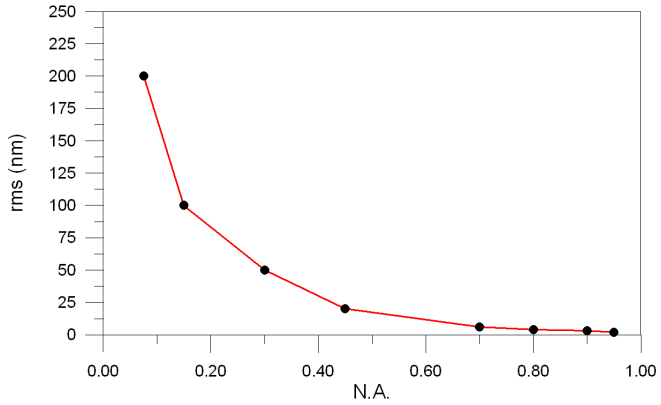

Figure 7.4.8 Dependence of the z-resolution of a confocal microscope with the Numerical Aperture.

The height resolving power is directly linked to the noise. The smallest roughness that can be measured is the noise of the instrument itself, while the smallest step height should be typically three times larger than the noise. Typical noise numbers for an objective with 0.95 Numerical Aperture are on the order of 1 nm. This should mean that the smallest step height, and thus the resolution, is on the order of 3 nm. Nevertheless, confocal image averaging can improve significantly the noise level at the cost of larger measuring time. Figure 7.4.9 shows the result of the measure of a 10 nm step height with 1 confocal image per plane (black line) and 10 confocal images averages per plane (red line).

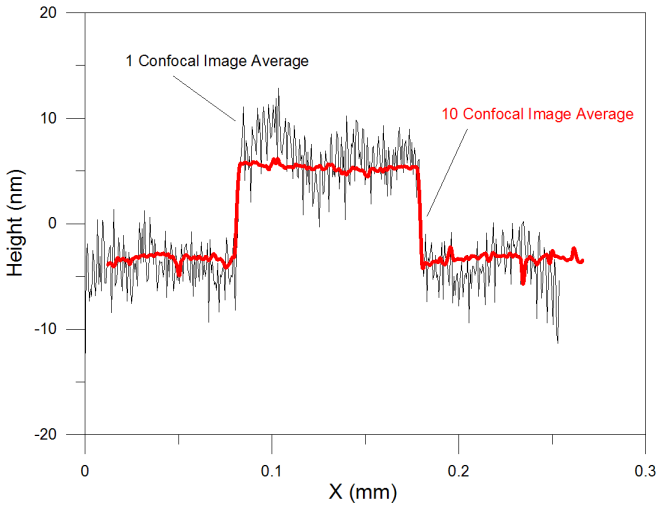

Figure 7.4.9 Measure of a 10 nm step height with a 50X 0.95NA objective. Black line with 1 confocal image per plane. Red line with 10 confocal images averaged per plane.

Averaging too many images will not improve indefinitely the noise. Mechanical stressing, small thermal variations, external vibration among other factors is limiting low frequency components that affect the calibration of the instrument. These low frequency components appear on the measure as waviness, and they are stable on a stabilized instrument within 1 minute. This practically limits the noise of a confocal instrument to the order of 0.3 nm, meaning that the smallest step height resolved is on the order of 1 nm.

Many commercial instruments claim to have 1 nm resolution but they tend to confuse the customer. Some of them are referring to the display resolution, which is the smallest number shown in the software. Others are referring to the resolution of the Optical Linear Scale of the vertical scanning device or to the capacitive sensor of the piezo, but not to the smallest resolved step height. A good practice to check the noise limit of the instrument is to ask to the manufacturer a measure of a flat mirror. The roughness of the mirror cannot be profiled by a confocal instrument, and what you will get is the noise of the instrument itself.

7.4.3 Errors in Imaging Confocal Microscopes

7.4.3.1 Objective's flatness error

Objective's manufacturers design the optics in a way to keep all the aberrations within the depth of field of the objective itself. This ensures that a normal use of the microscope, visually or with a camera, will not put in evidence small optical aberrations residual on the design like field curvature, spherical aberration, astigmatism or coma. Most of the optical correction is done on the objective itself, but some manufacturers are combining the lenses on the objective, the field lens, and the binocular to even get better optical correction at the end.

A three dimensional Imaging Confocal Microscope pushes the objective to its limits. The height resolution is close to 1 nm for the highest Numerical Aperture of 0.95, with a depth of field of 0.7 microns. This is hundreds of times higher resolution, which will show any non-corrected optical aberration present within the depth of field. The most affecting optical aberration is the spherical aberration. Figure 7.4.10 shows the spherical aberration of three typical objectives (20X, 50X and 100X) before instrument calibration. It is worth noting the decrease of the profile length due to the field of view of each objective.

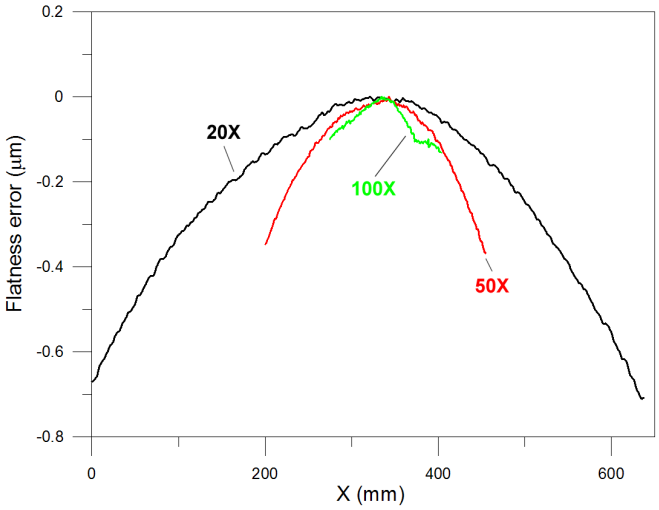

Figure 7.4.10 Optical aberrations before instrument calibration. Objectives 20X, 50X, and 100X.

7.4.3.2 Calibration of the flatness error

In order to deal with the optical aberrations an Imaging Confocal Microscope is calibrated. The most typical way to do such calibration is with a reference flat surface like a good quality mirror, most of the times provided by the manufacturer of the instrument. The mirror is placed under the microscope and tilted to a position as perpendicular to the optical axis as possible. The software takes a reference topography which is stored and automatically subtracted to any measure. The process is repeated for all objectives. Figure 7.4.11 shows the measure of a flat calibration mirror after the calibration procedure. It is also shown the effect of noise decrease with the magnification, which is normal with the increase of magnification (increase of Numerical Aperture).

It is highly recommended to do the calibration procedure with a stabilized instrument. Any mechanical stress present on the instrument, very normal after a system installation or any sudden temperature change, will make the calibration and the measure to have a mismatch. This mismatch will appear on the measure as low frequency components, increasing the instrument noise and making the instrument not useful for the measurement of flat and smooth surfaces.

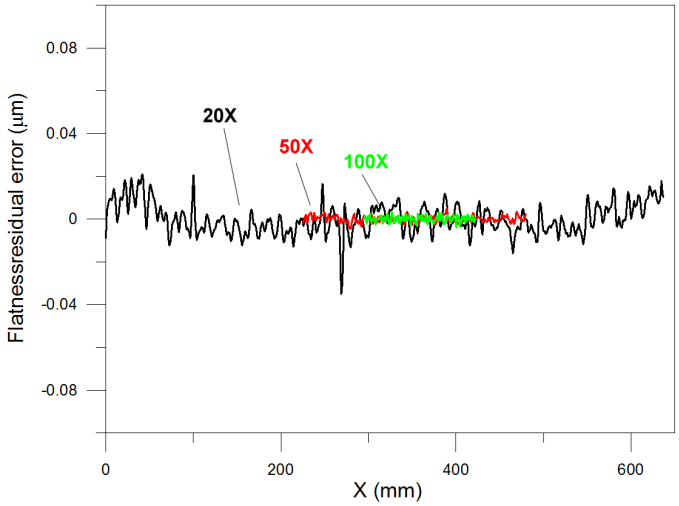

Figure 7.4.11 Residual profile of the optical aberrations after instrument calibration. Objectives 20X, 50X, and 100X.

7.4.3.3 Measurements on thin transparent materials

It is well known that Imaging Confocal Microscopes are insensible to dissimilar materials. Nevertheless, this is only true with optically opaque materials of for transparent materials that are optically resolved with the objective in use. When measuring step heights of transparent materials with thicknesses smaller than the depth of focus of the objective and the coherence length of the light source an additional effect appears: the light reflection on the top and the bottom parts of the transparent materials interfere with an interference state that depends on the wavelength, the thickness, the refraction index, and the Numerical Aperture of the objective. This interference shifts the peak of the axial response and consequently, the measured topography is not trustable.

This is a typical effect when measuring step height of Silicon Oxide on Silicon, with mismatch measurement with other instruments even on the same instrument with different objectives due to the change of the Numerical Aperture.

7.4.3.4 Optical roughness vs contact stylus

It is usual to compare roughness values of optical profilers with contact stylus profilers. Most of the times the values of both instruments do not coincide.

The tip of a contact stylus used for roughness measures is typically 2.5 micron radius and 60 or 90 degree angle. On optical profilers the equivalent tip radius is much smaller and the equivalent geometry is much sharper. On contact profilers

the real profile is convoluted by the tip, losing frequencies beyond the lateral resolution of the instrument. In contrast, the lateral resolution of optical profilers can be higher, profiling higher frequencies. The lateral resolution is dependent of the mean wavelength and the Numerical Aperture. For some optical combinations, the lateral resolution are nearly matching the contact stylus, and the roughness values are very similar. For high NA objectives the measured profile contains more detail than the equivalent contact profile, and the roughness value is typically higher.

In general, measures made with a 20X objective nearly mach roughness values with contact stylus. For smaller magnifications, the instrument noise increases and this could make the measured profile to contain false frequencies. For higher magnifications, more than 20X, it is needed to process the data in order to simulate the tip convolution. Figure 7.4.12 shows the measured profile with a 50X objective of a roughness standard of Ra=0.50 micron nominal roughness (black line) and the convolution with a mathematical sphere of 2.5 microns radius (red line). The roughness data is calculated over the convoluted data.

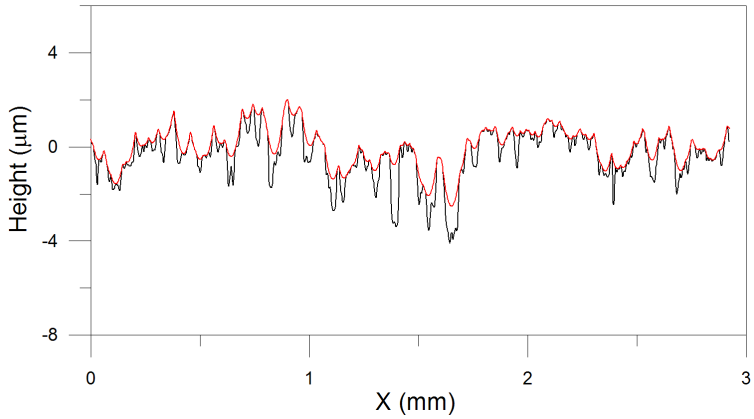

Figure 7.4.12 Measured profile with a 50X objective of a roughness standard (black line) and data convoluted with a sphere of 2.5 microns radius (red line).

Table 7.4.2 shows the results of the roughness values calculated over the profiles of figure 7.4.12. The nominal roughness is Ra=0.5 micron which coincides with the convoluted profile.

Table 7.4.2 Roughness values of the profiles of figure 4.12. Measured profile (left) and convoluted profile (right).

ISO 4287		
Amplitude parameters - Rougl		
Rp	1.67461	um
Rv	2.46702	um
Rz	4.14163	um
Rt	4.64758	um
Ra	0.800153	um
Rq	1.00055	um

ISO 4287		
Amplitude parameters - Rougl		
Rp	1.17792	um
Rv	1.49494	um
Rz	2.67286	um
Rt	3.20963	um
Ra	0.547086	um
Rq	0.669187	um

7.4.4 Lateral resolution

The lateral resolution of an Imaging Confocal Microscope is the highest that can be achieved with an optical instrument. As discussed in section 1.3.3.1, the lateral resolution is stated by the diffraction limit and equals to 0.61λ /NA, where λ is the mean wavelength and NA the Numerical Aperture of the objective. The lateral resolution increases by decreasing the mean wavelength or by increasing the Numerical Aperture. The highest NA objective in air is 0.95 and typical wavelength is on the violet – blue region (between 0.4 and 0.46 micron). This equals to lateral resolution between 0.25 and 0.29 micron.

Despite the lateral resolution is stated by the Rayleigh criteria of diffraction, confocal microscope manufacturers like to talk about the half of this limit. They use the Line and Space criteria (L&S) often used in the semiconductor industry. On that case, the minimum feature size during wafer inspection is the observation of gratings and equals to the half of the Rayleigh lateral resolution. If a grating is thought as a sinusoid, the cut-off frequency (highest frequency grating resolved) will equal to the diffraction limit corresponding to the optics in use. At the same time, the grating is composed by the line and its space, meaning that it is possible to resolve a feature size half of the frequency grating. With the L&S criteria, the lateral resolution of an Imaging Confocal Microscope decreases between 0.12 to 0.15 micron, depending on the mean wavelength in use.

Figure 7.4.13 shows the confocal image of a periodic structure of 0.4 micron period. The circular are has an average diameter of 0.2 micron.

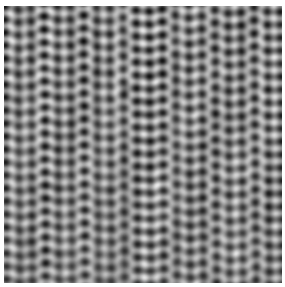

Figure 7.4.13 Confocal Image of a periodic structure of 0.4 micron period and 0.2 micron diameter.

Despite it is possible to revolve features around 0.15 micron with an Imaging Confocal Microscope it is much more difficult to precisely resolve the height of such features. On that case trustable results are more depending on the experience of the manufacturer to write the appropriate algorithms. Figure 4.14 shows the result of an AFM calibration standard measured with a 150X objective (0.95NA) and 0.46 micron mean wavelength.

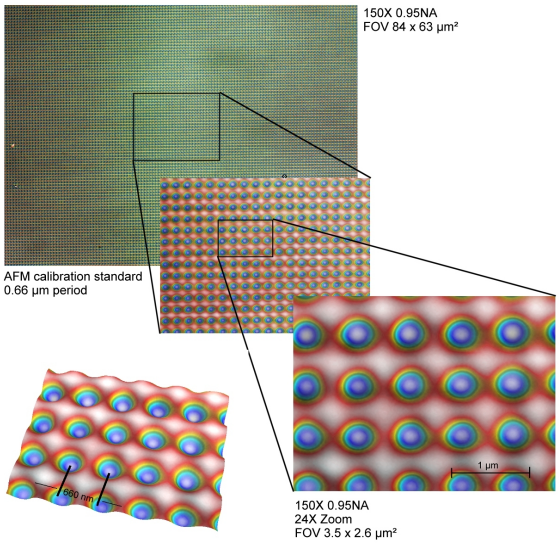

Figure 7.4.14 Measure of an AFM calibration standard with a Confocal Profiler with a 150X objective.

7.5 Thin and Thick Film with ICMs

7.5.1 Introduction

Confocal microscopy is a well-known technique for obtaining non-contact three-dimensional surface measurements. One advantage of these instruments is their ability to supply correct results on surfaces containing dissimilar materials without the need for any correction of the measurements. This feature makes the confocal profilers useful for applications such as biomedics, materials testing, chemistry and microelectronics.

However, one of the applications, which is considered to be very difficult to carry out with most optical imaging profilers is the measurement of stratified media. These media show refractive-index variations in the axial direction. Typical examples are integrated circuit architectures, integrated optics structures and optoelectronic devices.

7.5.2 Thick Films

Axial imaging is obtained in a confocal microscope by scanning the sample through the confocal depth of focus. For a thick film we obtain peaks in the axial response arising from reflection at the two parallel reflecting surfaces. The widths of the peaks are reduced when the NA of the objective increases and the distance between the peaks increases with the thickness of the film. Figure 7.5.1 shows the experimental axial responses of a 140-μm-thick glass sheet (n_1=1.52) obtained with a 10X 0.3NA objective.

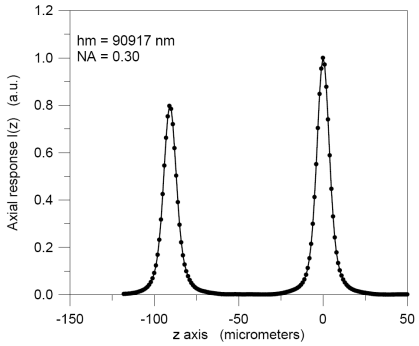

Figure 7.5.1 axial response of a 140 μm thick glass sheet.

The measured separation of the peaks h_m is very different from the real thickness h of the sheet because of two important factors: (i) depth distortion due to the index of refraction n of the medium and (ii) the spherical aberration caused by focusing with high NA optics through a refractive medium. The relationship between h_m and h can be predicted by a simple geometrical model:

$$\frac{h_m}{h} = \frac{\int_0^{\theta_0} \sin\theta d\theta}{\int_0^{\theta_0} \frac{\left(n^2 - \sin^2\theta\right)^{1/2}}{\cos\theta} \sin\theta d\theta} \tag{7.5.1}$$

where θ is the angle of incidence of a ray impinging on the layer surface and sin θ_0 is the NA of the objective.

Figure 7.5.2 shows the results of calculating the correction factor h_m/h for the thick glass sheet. Some experimental values obtained from the axial responses of Fig. 7.5.1 are also plotted. The agreement is fairly good for the lower NA objectives but is less satisfactory for NA values above 0.5. Differences between experimental and theoretical results may also be due to apodization and residual aberrations in the objectives.

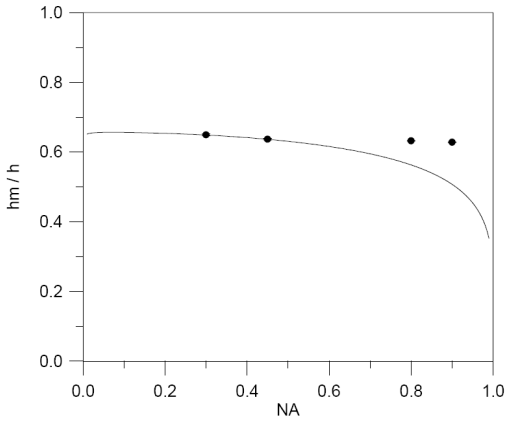

Figure 7.5.2 Relationship h_m/h as a function of the NA of the objective predicted by the simple geometrical model for a 140-µm-thick glass sheet (continuous line). Experimental values obtained from the axial responses are also plotted.

The geometrical model is also wrong when axial imaging is used to measure the thickness of thin layers. In these samples, the peaks obtained in the axial scanning are much closer, and effects such as multiple reflections and interferences between wavefronts reflected on the interfaces become very significant.

7.5.3 Thin Films

According to wave theory, in a confocal microscope the sample is illuminated by an angular spectrum of plane waves. Each of these components is reflected by the

structured surface with an amplitude reflection coefficient R(θ). The effect of the confocal aperture is to integrate over the amplitudes of the reflected angular spectrum. When the sample is scanned along the z axis, the detected intensity is given by:

$$I(z) = \left| \int_0^{\theta_0} R(\theta) P(\theta) \exp(2ikn_0 z \cos\theta) \sin\theta \cos\theta d\theta \right|^2 \tag{7.5.2}$$

where P(θ) is the pupil function, k is the wave number and n_0 is the refractive index of the medium surrounding the surface of the sample. If we consider a layer of refractive index n_1 on a substrate of refractive index n_s, the reflection coefficient R(θ) for linearly polarized illumination is given in terms of the reflection coefficients for parallel and perpendicular polarization by:

$$R(\theta) = (R_\sigma - R_\pi)/2 \tag{7.5.3}$$

Where

$$R_\sigma = \frac{R_{01,\sigma} + R_{1s,\sigma} \exp(2i\beta)}{1 + R_{01,\sigma} R_{1s,\sigma} \exp(2i\beta)} \tag{7.5.4}$$

and

$$\beta = kn_1 h \cos\theta_1 \tag{7.5.5}$$

and similarly for R_π, where:

$$R_{o1,\sigma} = \frac{n_0 \cos\theta - n_1 \cos\theta_1}{n_0 \cos\theta + n_1 \cos\theta_1}, \qquad R_{o1,\pi} = \frac{n_1 \cos\theta - n_0 \cos\theta_1}{n_1 \cos\theta + n_0 \cos\theta_1}$$

$$R_{1s,\sigma} = \frac{n_1 \cos\theta_1 - n_s \cos\theta_s}{n_1 \cos\theta_1 + n_s \cos\theta_s}, \qquad R_{1s,\pi} = \frac{n_s \cos\theta_1 - n_1 \cos\theta_s}{n_s \cos\theta_1 + n_1 \cos\theta_s} \tag{7.5.6}$$

Figures 7.5.3a and 7.5.3b show the axial response I(z) calculated from expression 7.5.2 for two layers of SiO_2 (n_1=1.46) deposited on a Si substrate (n_s=3.88) with thicknesses h of 1.5 μm and 1 μm respectively. The pupil function is P(θ)=1 (aberration-free objective), the NA is 0.9 and the light wavelength is 632.8 nm. In Fig. 7.5.3a the axial response shows two peaks: the smaller one, which appears in the position z=0 μm, comes from the reflection on the air-SiO_2 interface; the larger one, which appears in the position z=-0.847 μm, comes from the reflection on the SiO_2-Si interface. Because of the multiple reflections, some additional weaker peaks appear deeper in the z-scanning. The two main peaks are partially overlapped, but it is still possible to measure the distance h_m between them. The

situation is very different in Fig. 7.5.3b, where the two peaks cannot be resolved, and it is therefore not possible to assign any h_m value to this axial response.

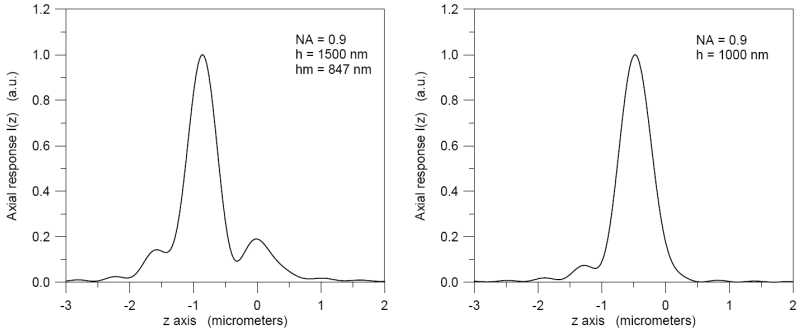

Figure 7.5.3 Axial responses I(z) calculated from expression (D.2) for a layer of SiO_2 (n_l=1.46) deposited on a Si substrate (n_s=3.88). Thicknesses of the layers are 1.5 µm (a) and 1 µm (b). NA is 0.90 and the light wavelength is 632.8 nm

Figure 7.5.4 show the relationship between the separation of the peaks h_m predicted by expression 7.5.2 and the real thickness of the layer h for NA of 0.9. For comparison, the results obtained from expression 7.5.1 are also plotted (dashed lines). Three main factors can be noted:

- The wavy behavior of the h_m/h relationship caused by interferences between wavefronts reflected at the layer interfaces.

- The lack of continuity of the h_m/h relationship for h values smaller than 2 µm. From the axial responses calculated from expression 7.5.2, it is observed that the z-position of the larger peak coming from the reflection on the SiO_2-Si interface oscillates slightly when the thickness of the layer h increases. However, the small peak coming from the reflection on the air-SiO_2 interface oscillates with much larger amplitude in such a way that sometimes it even becomes embedded in the larger peak. Of course, in these conditions it is not possible to assign any h_m value to the axial response.

- The existence of a limit of resolution in the layer thickness measurement, which is reached when the two peaks of the axial response become unresolved. Even when one is using microscope objectives with high NA, this limit of axial resolution turns out to be very close to layer thicknesses h of 1.5 µm or above. This is the situation reproduced in Fig. 7.5.3a, where the overlapping of the two peaks is very close to the limit given by the generalized Rayleigh criterion.

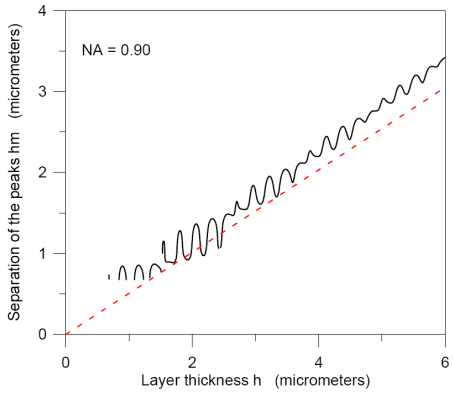

Figure 7.5.4 Relationship between the separation of the peaks h_m predicted by expression D.2 and the real thickness h of a layer of SiO_2 (n_l=1.46) deposited on a Si substrate (n_s=3.88). NA is 0.90 and light wavelength is 670 nm. Red line: linear regression.

Unfortunately, the limit of resolution seems to mean that confocal technology is unable to measure the shape of structured surfaces such as those obtained when developing integrated circuits, integrated optics, MEMs and optoelectronic devices. These samples are obtained by the growth or the deposition of various layers of dissimilar materials (Si, SiO_2, Si_3N_4, photoresists, etc) with thicknesses close to or well under 1 μm. After the deposition, the layers are patterned by well-known photolithographic processes, thus providing different layouts.

7.6 Case study: roughness prediction on steel plates

This example will illustrate how an Imaging Confocal Microscope is used for the assessment of key parameters on steel industry. During the manufacturing of steel plates for automotive and aero-space applications, the flat and smooth plate is processed with the intention to change its surface texture. One of the main processes is the increase of the roughness in a very well controlled way. Roughness will have a direct impact with paint adhesion. Too many smooth surfaces will have low paint adhesion, while higher roughness surface will have better adhesion. Nevertheless, random roughness can create a waviness effect on the upper layers of the paint, creating a visual effect that makes the final customer of a car to feel low cost surface finish. What steel manufacturers do is to press the steel plate against a roll. The roll has a manufactured surface texture in a way that after pressing the steel plate will imprint on it the desired roughness and texture. Such texture increases the effective adhesion area by creating craters and keeping a flat upper region.

Figure 7.6.2 shows the surface texture of one of such rolls manufactured with Electron Beam Discharge (EBD) technology. A steel roll is introduced into a vacuum chamber and each one of the electron discharges creates a crater-like structure. The measure of the surface was done with a 20X objective and field stitching. Approximately, each field of view of the objective was measuring about 4 craters. There were needed 6x6 single fields spanning a total area of 3.5 x 3.5 mm^2.

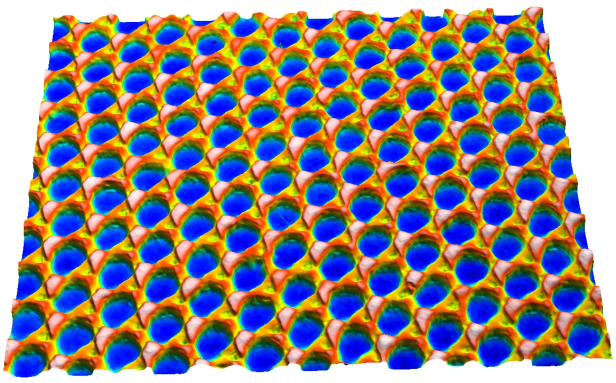

Figure 7.6.1 Texture of steel roll after EBD texturing process.

Under a certain amount of pressure between the roll and the steel plate, only 70% of the highest texture points of the surface are imprinted. Figure 7.6.2 shows the Bearing Area curve of the previous surface. The predicted roughness on the final steel plate will be calculated by cutting the surface at 70% of its bearing area point and inverting the result.

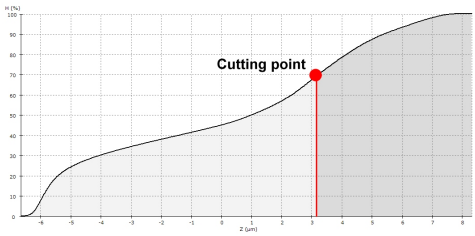

Figure 7.6.2 Bearing Area curve of the surface of figure ??. The cutting point for the prediction of the surface is located at 70% of the highest point.

Figure 7.6.3 shows the result of cutting the surface at the mentioned point and inverting the result. The surface roughness of the original roll surface and the predicted surface are also shown.

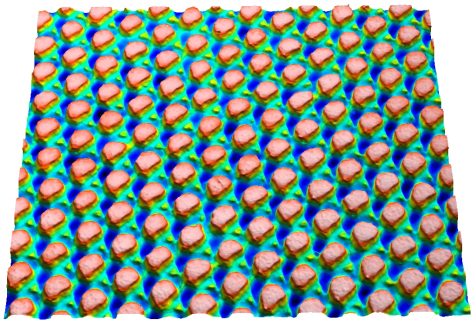

Figure 7.6.3 Predicted surface after pressing a steel roll on a steel plate.

Table 6.1 Predicted surface roughness parameters of the original roll surface (left) and the predicted steel plate surface (right).

Original surface roughness parameters

ISO 25178			
Height Parameters			
Sq	4.60269	µm	*Root mean square height*
Sp	7.94633	µm	*Maximum peak height*
Sv	8.40269	µm	*Maximum pit height*
Sz	16.3490	µm	*Maximum height*
Sa	4.20629	µm	*Arithmetic mean height*

Predicted surface roughness parameters

ISO 25178			
Height Parameters			
Sq	3.98593	µm	*Root mean square height*
Sp	6.39672	µm	*Maximum peak height*
Sv	3.96401	µm	*Maximum pit height*
Sz	10.3607	µm	*Maximum height*
Sa	3.73933	µm	*Arithmetic mean height*

7.7 References

R. Artigas, A. Pintó, and F. Laguarta, "*Three-dimensional micromeasurements on smooth and rough surfaces with a new confocal optical profiler*", **in the Optical Measurement systems for industrial inspection**, Vol. 3824, pp 93-103, Munich (1999).

R. Artigas, F. Laguarta, and C. Cadevall. "*Dual-technology optical sensor head for 3D surface shape measurements on the micro and nano-scales*". Spie Vol 5457, 166-174 (2004).

M. R. Atkinson, A. E. Dicson, and S. Damaskinos. "*Surface-profile reconstruction using reflection differential phase-contrast microscopy"*, **Applied Optics**, Vol. 31, No. 31, pp. 6765-6771. (1992).

J. Bennett, and L. Mattson. "*Introduction to surface roughness and scattering*", **Optical Society of America** (Washington, 1989).

G.J. Brakenhoff, H.T.M. van der Voort, E.A. van Spronsen, and N. Nanninga, "*3-Dimensional imaging of biological structures by high resolution confocal scanning laser microscopy*", **Scanning micros. 2**, 33-40 (1978).

E. Botcherby, M. Booth, R. Juškaitis, and T. Wilson. "*Real-time slit scanning microscopy in the meridional plane*". **OPTICS LETTERS** / Vol. 34, No. 10 / May 15 (2009).

C. Cadevall, R. Artigas, and F. Laguarta. "*Development of confocal-based techniques for shape measurements on structured surfaces containing dissimilar materials*". Spie Vol 5144, 206-217 (2003).

S. Cha, P. C. Lin, L. Zhu, E. L. Botvinick, P. Sun. "*3D profilometry using dynamic configurable confocal microscope" (fill out).*

S. Cha, P. C. Lin, L. Zhu, P. Sun, and Y. Fainman. "*Nontranslational three-dimensional profilometry by chromatic confocal microscopy with dynamically configurable micromirror scanning*". **APPLIED OPTICS** Vol. 39, No. 16 (2000).

J-A. Conchelo, and E. W. Hansen. "*Enhanced 3-D reconstruction from confocal scanning microscope images. 1: Deterministic and maximum likelihood reconstructions"*, **Applied Optics,** Vol. 29, No. 26, pp. 3795-3804. (1990).

R. G. Dorsch, G. Häusler, and J. M. Herrmann. "*Laser triangulation: fundamental uncertainty in distance measurement"*, **Applied Optics,** Vol. 33, No. 7, pp. 1306-1314. (1994).

D. T. Fewer, S. J. Hewlett, and E. M. McCabe. "*Influence of source coherence and aperture distribution on the imaging properties in direct view microscopy"*, **J. Opt. Soc. Am. A**, Vol. 14, No. 5, pp. 1066-1075. (1997).

R. Fiolka, A. Stemmer, and Y, Belyaev. "*Virtual slit scanning microscopy"*. **Histochem Cell Biol.** 128:499-505 (2007).

D. G. Flagello, T. Milster, and A. E. Rosenbluth. "*Theory of high NA imaging in homogeneous thin films"*. **J. Opt. Soc. Am.** Vol 13, N-1 (1996).

M. Gu, and C. J. Sheppard. "*Effects of defocus and primary spherical aberration on three-dimensional coherent transfer functions in confocal microscopes"*, **Applied Optics,** Vol. 31, No. 14, pp. 2541-2549. (1992).

Q. S. Hanley, P. J. Verveer, M. J. Gemkov, D. Arndt-Jovin & T. M. Jovin. "*An optical sectioning programmable array microscope implemented with a digital micromirror device*". **Journal of Microscopy**, Vol. 196, Pt 3 (1999).

M. Ishihara, and H. Sasaki. *"High Speed surface measurement using a nonscanning multiple-beam confocal microscope"*. **Opt. Eng.** 38 (6) 1035-1040 (1999).

D. Karadaglic. "*Image formation in conventional brightfield reflection microscopes with optical sectioning property via structured illumination*", **Micron** 39 302–310 (2008).

S. Kimura, and C. Munakata. "*Depth resolution of the fluorescent confocal scanning optical microscope"*, **Applied Optics**, Vol. 29, No. 4, pp. 489-494. (1994).

F. Laguarta, R. Artigas, A. Pintó, and I. Al-Khatib, "*Micromeasurements on smooth surfaces with a new confocal optical profiler"*, in the **three dimensional imaging, optical metrology and inspection IV,** Vol. 3520, pp 149-160, Boston. (1998).

C.H. Lee, H. Chiang, and H. Mong. "*Sub-difraction limit imaging based on the topographic contrast of differential confocal microscopy"*. **Optics Letters** / Vol. 28, No 19 (2003).

P.C. Lin, P. Sun, L. Zhu, and Y. Fain,am., "*Single-shot depth-section imaging through chromatic slit-scan confocal microscopy*", **Applied Optics**, Vol. 37, No. 28, pp 6764-6770. (1998).

D. Malacara, *Optical Shop Testing*, (John Wiley & Sons, Inc. 1992).

M. A.A. Neil, R. Juskaitis, and T. Wilson. "*Method of obtaining optical sectioning by using structured light in a conventional microscope*". **OPTICS LETTERS** / Vol. 22, No. 24 (1997).

V. Poher, H. X. Zhang, G. T. Kennedy, C. Griffin, S. Oddos, E. Gu, D. S. Elson, J. M. Girkin, P.M.W. French, M.D. Dawson, and M.A.A. Neil. "*Optical sectioning microscopes with no moving parts using a micro-stripe array light emitting diode*". **OPTICS EXPRESS** , Vol. 15, No. 18 (2007).

V. Poher, G. T. Kennedy, H. B. Manning, D. M. Owen, H. X. Zhang, E. Gu, M. D. Dawson, P. M. W. French, and M. Neil. "*Improved sectioning in a slit scanning confocal microscope*". 2008 / Vol. 33, No. 16 / **OPTICS LETTERS**.

L. H. Schaeffer, D. Schuster, & J. Schaefer. "*Structured illumination microscopy: artefact analysis and reduction utilizing a parameter optimization approach*". **Journal of Microscopy**, Vol. 216, Pt 2 (2004).

C. J.R. Sheppard, and X. Q. Mao. "*Confocal microscopes with slit apertures"*, **Journal of Modern Optics**, Vol. 35, No. 7, pp. 1169-1185. (1988).

C. J.R. Sheppard, and D. M. Shotton, "C*onfocal laser scanning microscopy*", BIOS Scientific Publishers, Oxford (1997).

C. J.R. Sheppard. "*Binary optics and confocal imaging"*, **Optics Letters,** Vol. 24, No. 8, pp. 505-506. (1999).

C. J.R. Sheppard, T. J. Connolly, Jin Lee, and C. J. Cogswell. "*Confocal imaging of a stratified medium"*. **Applied Optics**. Vol 33, N-4 (1994).

P. J. Smith, C. M. Taylor, A. J. Shaw, and E. M. McCabe. "Programmable array microscopy with a ferroelectric liquid-crystal spatial light modulator". **APPLIED OPTICS** y Vol. 39, No. 16 (2000).

Stamnes J., *Waves in focal regions* (IOP Publishing ,Boston, 1986).

T. Tanaami, S. Otsuki, N. Tomosada, Y. Kosugi, M. Shimizu, and H. Ishida. "*High-speed 1-frame_ms scanning confocal microscope with a microlens and Nipkow disks*". **APPLIED OPTICS** Vol. 41, No. 22 (2002).

H. Tiziani, M. Wegner, and D. Steudle. " *Confocal principle for macro- and microscopic surface and defect analysis"*. **Society of Photo-optical instrumentation Engineers.** [S0091-3286(00) 0301-9].

P.J. Verveer, and T. M. Jovin. "*Improved restoration from multiple images of a single object: application to fluorescence microscopy"*, **Applied Optics,** Vol. 37, No. 26, pp. 6240-6246. (1998).

P.J. Verveer, Q. S. Hanley, P. W. Verbeek, L. J. Van Vliet, and T.M. Joven. "*Theory of confocal fluorescence imaging in the Programmable Array Microscope (PAM)"*. **Journal of Microscopy** / Vol. 189 Pt 3 (1998).

G. Q. Xiao, T. R. Corle, and G. S. Kino. "*Real time confocal scanning optical microscope"*, **Applied Physics Letters**, Vol. 53, No. 8, pp. 716-718. (1988).

R. Webb, and F. Rogomentich. "*Confocal microscope with large field and working distance"*, **Applied Optics,** Vol. 38, No. 22, pp. 4870-4875. (1999).

T. Wilson, and A.R. Carlini, "*Depth discrimination criteria in confocal optical systems*", **Optik 76**, pp. 164-166. (1987).

T. Wilson, *Confocal microscopy*, (Academic, London, 1990).

T. Wilson, and B. Masters. "*Confocal microscopy"*, **Applied Optics**, Vol. 33, No. 4, pp. 565-566. (1994).

T. Wilson, R. Juskaitis, A.A. Neil, and M. Kozubek. "*Confocal microscopy by aperture correlation"*. **Optics Letters** / Vol 21, No 23 (1996).

M. Wuatanabe, S. K. Nayar, and M. Noguchi. "*Real time computation of depth from focus"*. **Proc. SPIE**, Vol. 2599, pp. 14-25.